TJ201 72-157

本資料は413年 7月31日付けで登録区分変更する。

〔技術情報グループ〕

COMPILATION

OF

FAST CRITICAL EXPERIMENTS

FOR

ANALYSIS OF DOPPLER EXPERIMENTS

[redacted]

Compilation of Fast Critical Experiments

(SEFOR)

Analysis of Doppler Experiment (I)

Editors

Y. Matsuno, S. Iijima, T. Kamei,

M. Iida, T. Yoshida, T. Ugajin

May 31, 1972

The work performed under the contract with the
Power Reactor and Nuclear Fuel Development Corporation

Tokyo Shibaura Electric Company, Ltd.

The work done at

NAIG Nuclear Research Laboratory

Suehiro-cho 250, Kawasaki-shi, Kawasaki-ku

Japan

J201 72-15

高速臨界実験データの収集

—SEFOR—

ドップラー実験データの解析（I）

高速増殖炉の核特性および安全性に関するデータを得るために，各国研究機関において高速臨界実験装置が設置され，多種にわたる大量の測定値の蓄積が行なわれている。ドップラー反応度効果に関する実験も，その例にもれず，各国の高速臨界装置で精力的に行なわれているが，その多くは集合体中心で試料を加熱昇温して，それによる反応度変化を測定するという方式を採用している。

SEFOR(Southwest Experimental Fast Oxide Reactor)は，従来の臨界実験では不十分であった体系全体のドップラー反応度効果の研究を主要な目的の一つとして建造された高速実験炉で，臨界到達以来これまでに行なわれた実験から数多くのデータが公表されている。

本作業はこれまでに公表されたドップラー反応度効果に関する実験データをTable 1の項目に従って利用し易い形式に整理編集し，解析研究の便に供することを目的とする。さらに，解析の一例としてG.E社による解析結果を各項目の最後に付記して解析手法の目安をつけるのに便利なように配慮してある。

Table 1の分類では，たとえば，5.1－SEFOR－1はSEFOR才1炉心(SEFOR I)の中心反応率（5.1）を意味する。この分類番号が実験項目ごとに各ページの上端に印刷してあり，全体はルーズ・リーフ形式のファイルとなっている。したがって，使用者は任意に内容を差替えたり追加したりできるようになっている。

SEFOR才1炉心には測定上の要請からI－A～I－Jの8個のversionがあり，それぞれの特徴に適合した実験が行なわれている。各versionで行なわれた実験項目を一括してTable 2に示す。

対象とした文献は主としてGEAP Reportである。編集の際は編者の意見は一切挿入せず，原文章のまま収録した。利用者は確実を期するためできるだけ引用文献に立戻られることをお勧めする。

終りにPNCの金城氏に収集のプランニングについての討論をして頂いたことに対して謝意を表明する。

1972年5月31日

担当責任者：羽田幹夫*)
編集者：松野義明**)
飯島俊吾**)
亀井孝信**)
飯田正明**)
吉田正**)
宇賀神孝**)

*) 東京芝浦電気株式会社　動力炉開発部
**) 日本原子力事業株式会社NAIG総合研究所

INTRODUCTION

Many fast critical assemblies have been built in many countries in the world in order to accumulate valuable data about the nuclear characteristics and safety of the fast breeder reactor. The experiments about the Doppler reactivity effect are also not the exceptional case and hence are performed energetically at every research laboratory. However, almost all the measuring methods so far employed have been the sample Doppler reactivity methods, namely, those to determine the reactivity worth difference of a hot sample located at the center of a core from the same sample at the same location but in cold situation.

SEFOR (Southwest Experimental Fast Oxide Reactor) is an experimental fast reactor, one of the main purposes of which is the study of the whole core Doppler reactivity effect which has not been enough studied up to now on the fast critical assemblies, and a lot of data obtained from the experiments performed on SEFOR have been published.

The purpose of the present work is to collect and compile the data published so far according to the items indicated in Table 1 and to serve the convenience of the theoretical analysis. In addition, the analytical results of the General Electric Co. will be, as an example of analysis, added at the end of every item.

An expression 5.1-SEFOR-1 in the classification in Table 1, for example, represents the information about the central reaction rate (5.1) on the SEFOR core I. This identification is printed at the top of every page, corresponding to the experimental item informed on the page. This file has a form of loose-leaf for convenience and so the user could arbitrarily replace or add some pages.

SEFOR core I has eight versions from the experimental requirement, i.e. I-A ∿ I-J, and the measurements were made on suitable versions of the core I, corresponding to their characteristics, which are tabulated in Table 2.

Literatures we have mainly refered were the GEAP Reports. In this work we have never mixed our own opinions and only compiled the data as they were reported. We recommend the user of this file to look up the references to make sure the details.

To Mr. K. Kinjo of PNC we owe valuable discussions about planning of this work.

Editors: Y. Matsuno, S. Iijima,
T. Kamei, M. Iida,
T. Yoshida, T. Ugajin

Table 1

Table of Contents

Table 1 (cont'd)

Section 13. Control Rod Worth

Section 14. Neutron Importance

Section 15. Analytical References

15-SEFOR-1

Section 16. Experimental References

16-SEFOR-1

Table 2. List of measurements made on each version of SEFOR I

Exp. Item / Assembly	Criticality	Shape Factor	Reactivity Worth				Reaction Rates		Reactivity Coeff.				Heterogeneity							Spectra	Lifetime		Control Rods	Importance	Anal. References	References	Remarks
									Na Void	Doppler	Temperature	Other ρ	Activation	Reactivity	Coefficients	Reaction Rates	Worths	Lifetime	Leakage								
	2	3	4.1	4.2	4.3	4.4	5.1	5.2	6	7	8	9	10.1	10.2	10.3	10.4	10.5	10.6	10.7	11	12.1	12.2	13	14	15	16	
I-A	x																										Inherent Neutron Source Effect Measurement
I-B	x		x	x																			x		x	x	Including worth of fuel, B_4C & SUS rod worth
I-C	x																								x	x	
I-D	x		x	x			x	x			x	x									x		x		x	x	INS ℓ/β (noise)
I-E	x									x	x	x											x		x	x	Reflector worth Flow & Pressure Coeff.
I-F	x																						x				Fine reflector calib. Reactivity flow coeff.
I-I	x											x															
I-J	x									x	x	x															

1 - SEFOR-1 SEFOR (Southwest Experimental Fast Oxide Reactor)

Location: Arkansas, U.S.A.

Operated by: U.S. Atomic Energy Commission, Southwest Atomic Energy Associates, Karlsruhe Laboratory of West-Germany, EURATOM and the General Electric Company

Date of First Operation:

Basic Description:

The Southwest Experimental Fast Oxide Reactor (SEFOR) is a 20 MW(t) fast spectrum reactor fueled with mixed PuO_2 - UO_2 and cooled with sodium. SEFOR has characteristics similar to the large, soft spectrum fast breeder reactors fueled with mixed PuO_2 - UO_2 and is being used to obtain physics and engineering data at fuel compositions, temperatures, and crystalline states characteristic of power reactor operating conditions. SEFOR is particularly designed for the systematic determination of the Doppler coefficient of reactivity at temperatures up to the vicinity of fuel melting.

This reactor is controlled by the radial nickel reflector. The reflector will be divided into ten segments, which can be raised or lowered vertically to give the desired control. (see Fig. 1) Upper and lower reflectors consist of 4-in. nickel end plugs, which fit inside the fuel cladding.

The SEFOR core contains 108 fuel assemblies, each loaded into a hexagonal channel. The mean cell diameter is 3.160 in. across the flats, and the fuel region approximates a 34-in.-diam right circular cylinder. The core volume is 528.1 liters. Each fuel assembly contains six stainless steel-clad fuel rods, one in each corner of the hexagonal channel. The active fuel section, which consists of 0.875-in.-diam stacked PuO_2 - UO_2 pellets, is 33.81 in. long. At the center of fuel assembly there is a thin walled, stainless steel tightener sleeve and a 0.777-in.-diam BeO rod. At the periphery of the assembly are six 0.250-in.-diam stainless steel side rods. Besides normal fuel assemblies some assemblies containing guinea pig rod and/or B_4C rod in stead of normal fuel rods and the instrumented fuel assembly are prepared for special measurement or reactivity adjustment.

Core Element Description:

(1) General: The SEFOR core structure is made up of 109 hexagonal

tubular channels that are clamped around the periphery to form a bundle approximately 34.7 inches in diameter and 106 inches long. A plan view of the core structure is shown in Figure 1.

(2) Significant Data: Significant information on the core element components follows:

(i) Core Dimensions

Equivalent Diameter	34.7 in.
Cumulative Fuel Length	33.812 in.
Core Height (including axial gap and UO_2 insulators)	36-9/16 in.

(ii) Core Element

Maximum Number in Core	109
Calculated Weight	124 lb.
Fuel Rods per Core Element	6
Tightener Rods per Core Element	1
Rod Pitch	1.095 in.

(iii) Fuel Channel

Material	Type 304 SS
Shape	Hexagonal
Outside dimension across flats	3.150 ± 0.003 in.
Wall Thickness	0.060 ± 0.002 in.
Tubing Length	105 in.
Overall Length	106 in.
Side Rod Diameter	0.250 ± 0.001 in.
Weight	22 lb.

(iv) Fuel Rod

Weight (excluding Extension Rod)	11.0 lb.
Overall Length (standard rods)	49-5/8 in.
(special rods)	49-11/16 in.
Diameter	0.972 in.
Fuel Length	33.812 in.
Overall Core Length (including insulator and void)	36-9/16 in.
Number of Axial Segments	2
Cladding	
Material	Type 316 SS
Inside Diameter	0.890 ± 0.0015 in.
Wall	0.041 ± 0.0025 in.
Fuel Pellets	
Material	PuO_2 - UO_2

1 - SEFOR-1 (cont'd)

Diameter	0.875 ± 0.001 in.
Length	5/8 ± 3/32 in.
Density (based on pellet OD)	
% of theo.	92.6 ± 2
gm/cc	10.2
Density (based on cladding ID)	
% of theo.	89.5
gm/cc	9.85
Composition	PuO_2 - UO_2
Pu (239+241)/Pu+U	
standard rods	18.7%
special rods (Guinea Pig)	25.0%
Insulator Pellets	
Material	Depleted UO_2
Diameter	0.883 ± 0.001 in.
Length	3/8 in.
Density	
% of theo.	92
gm/cc	10.1
Reflector (upper & lower)	
Material	Nickel-ASTM-B160
Diameter	0.875 +0.000 -0.007 in.
Length	3-31/32 in.

(v) Extension Rod

Overall Length	64-27/32 in.
Weight	
Standard	4.12 lb.
Special	5.83 lb.
Cladding	
Material	Type 316 SS
Outside diameter	0.857 ± 0.005 in.
Wall	0.040 ± 0.005 in.
OD at spring contact points	0.970 ± 0.005 in.
Shielding	
Material	
standard	B_4C
special	50% B_4C & 50% SST. shot
min. density of B_4C (stand'd)	1.7 gm/cc
Length	54 in.
Min. weight	
standard	1.68 lb.
special (contains steel shot)	3.7 lb.

(vi) Tightening Rod

Overall Length	111-27/32 in.
Weight	10.0 lb.
Diameter	0.875 ± 0.002 in.
Cladding	
Material	Type 316 SS
Outside diameter	0.875 ± 0.002 in.
Wall	0.040 ± 0.002 in.
BeO Rod	
Material	Sintered BeO pellets
Diameter	0.777 +0.000 -0.003 in.
Overall length	36-9/16 in.
Density	2.9 gm/cc
Shielding	
Material	50% B_4C & 50% steel shot
Min. effective density	3.75 gm/cc
Min. weight	3.9 lb.
Length	56 in.
Reflector	
Material	Nickel-ASTM-B160
Diameter	0.780 +0.005 -0.000
Length (upper)	3-31/32 in.
Length (lower)	3-31/32 in.

(vii) Tightener Sleeve

Overall Length	110-1/8 in.
Tube Material	Type 304 SS
Spring material	Inconel 718
Spider material	Type 304 casting
Weight	5.3 lb.

(3) Fuel Rod: The SEFOR fuel rod is shown in Fig. 3. The fuel is divided into two segments to reduce the axial reactivity expansion coefficient by reducing the change in radial neutron leakage with changes in fuel temperature (steady state power level).

(4) Rod Compositions: The homogenized composition of the various rods which are inserted into the core from time to time are summerized in Table 3 and the composition of the unit cells and the over-all reactor model given in Table 4 and 5. The material densities corresponding to this reactor model are given in Table 6.

(5) Special Core Rods: The experimental program requires several special types of rods which will be placed in fuel positions in the core.

(i) Poison Core Rods

Rods filled with boron carbide which are identical to fuel rods except the core region contains a measured amount of B_4C powder compacted to 50% of theoretical density and a steel rod to occupy the remaining volume.

(ii) Practice Core Rods

These rods contain a stainless steel rod in the core and reflector regions.

(iii) UO_2 Core Rods

Uranium-dioxide core rods contain depleted UO_2 pellets in the core region.

(iv) Foil Holder Rods

These rods will contain foils used for physics measurements, and can be disassembled remotely for foil removal. These rods will only be used during wet critical testing.

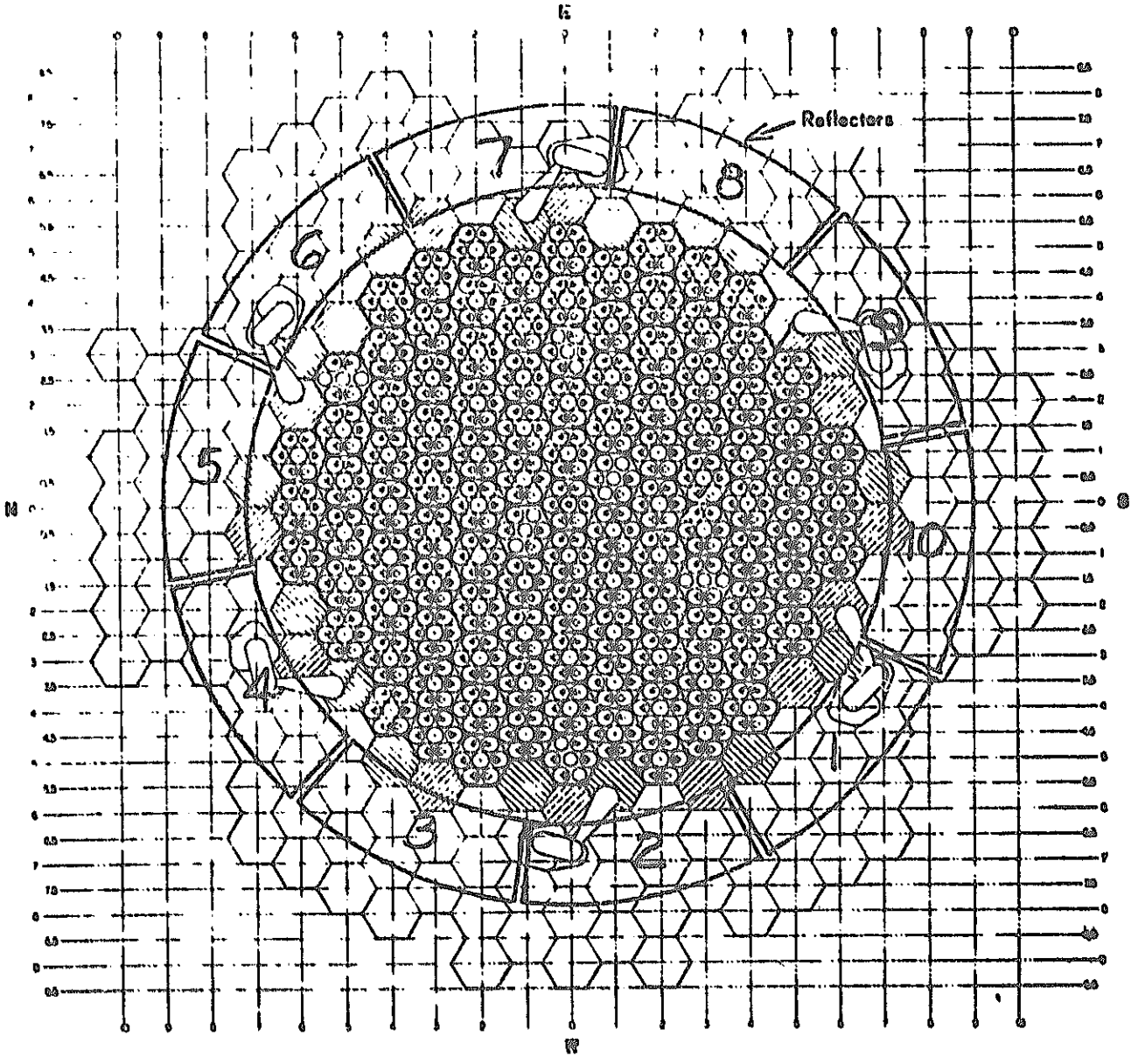

FIGURE 1. CORE LOADING LOCATIONS

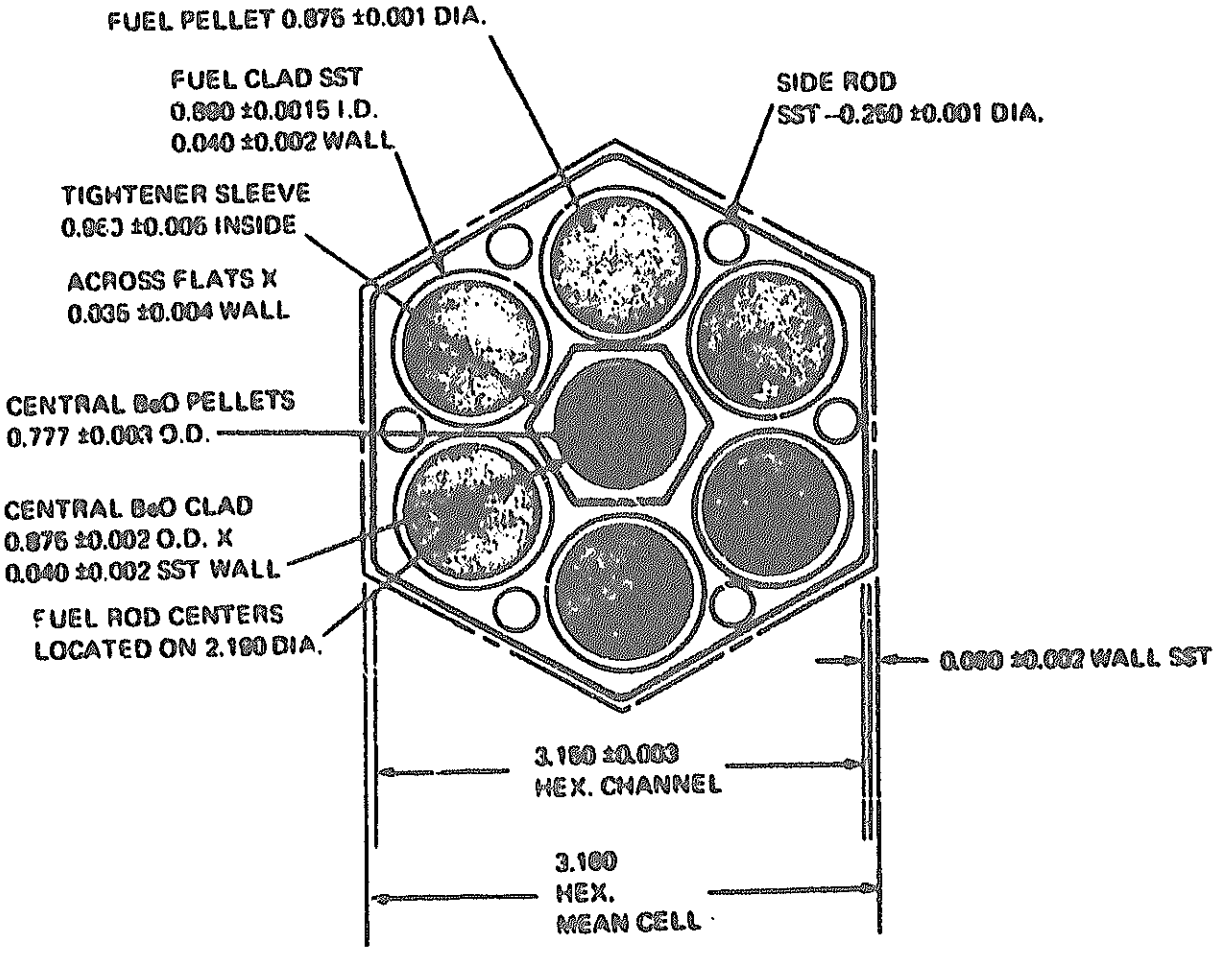

FIGURE 2. SEFOR FUEL CHANNEL

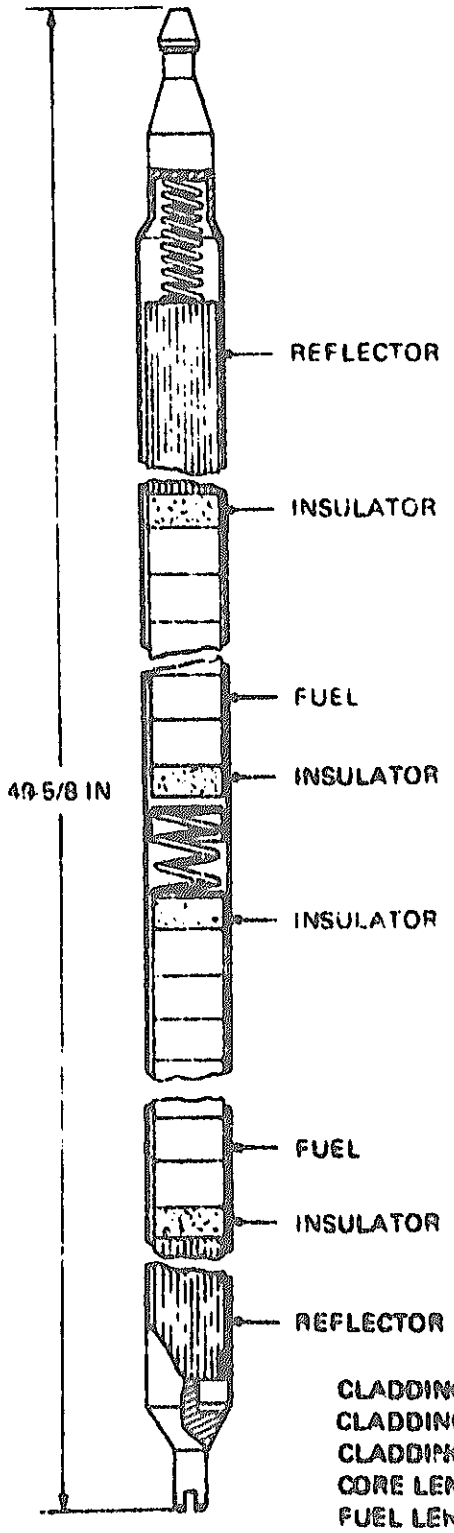

CLADDING O.D.	0.070
CLADDING MATL	STN. STL.
CLADDING THICKNESS	0.040
CORE LENGTH	36.56
FUEL LENGTH	33.81

FIGURE 3. SEFOR FUEL ROD

References:

1. L.D. Noble et al., GEAP-13588 (March, 1970) p.8G, pp.167-168

2. R.A. Meyer et al., GEAP-13598 (June, 1970) Section II pp.1-9

3. R.L. McVean et al., ANL-7248 (March, 1967) pp.10-11

2 - SEFOR-1 SEFOR (Southwest Experimental Fast Oxide Reactor)

Type of Experiment: Critical

General Description:

Experiments were performed on five major different core loadings, or arrangements, of fuel, BeO and B_4C rods within the core. These five different core loadings have been designated Assembly I-A through Assembly I-E, which are illustrated in figures 1 through 5.

In addition, a fine reflector was calibrated on other loading, Assembly I-F. A portion of the reactivity flow coefficient measurements were performed on Assembly I-I. The latter two loadings are shown in Figures 6 and 7. After initial operation at 10 MW with the assembly I-I, the core loading was changed to provide additional reactivity to offset the reactivity feedback introduced by operation at higher power levels. The change in loading was made by replacing a B_4C rod in core location W3.0-S2.0E with a stainless steel rod. The new core loading was designated Assembly I-J, the illustration of which is shown in reference 3.

The reactivity worth of fuel, B_4C and stainless steel rods were measured at four different radial core locations in Assembly I-B. During this measurements and in subsequent investigations it was revealed that a number of the fuel rods in this core were as much as 40% low in reactivity worth when compared to a standard rod. These very low worth fuel rods were removed and the core size was reduced by replacing fuels from the core boundary. The actual SEFOR minimum critical core loading thus obtained was 522 PuO_2 - UO_2 fuel rods and 100 BeO tightener rods (Assembly I-C).

Date:

Critical Configurations:

Figures 1 through 7 illustrate the top views of Assemblies. A typical side view of the Assembly will be shown in Figure 8.

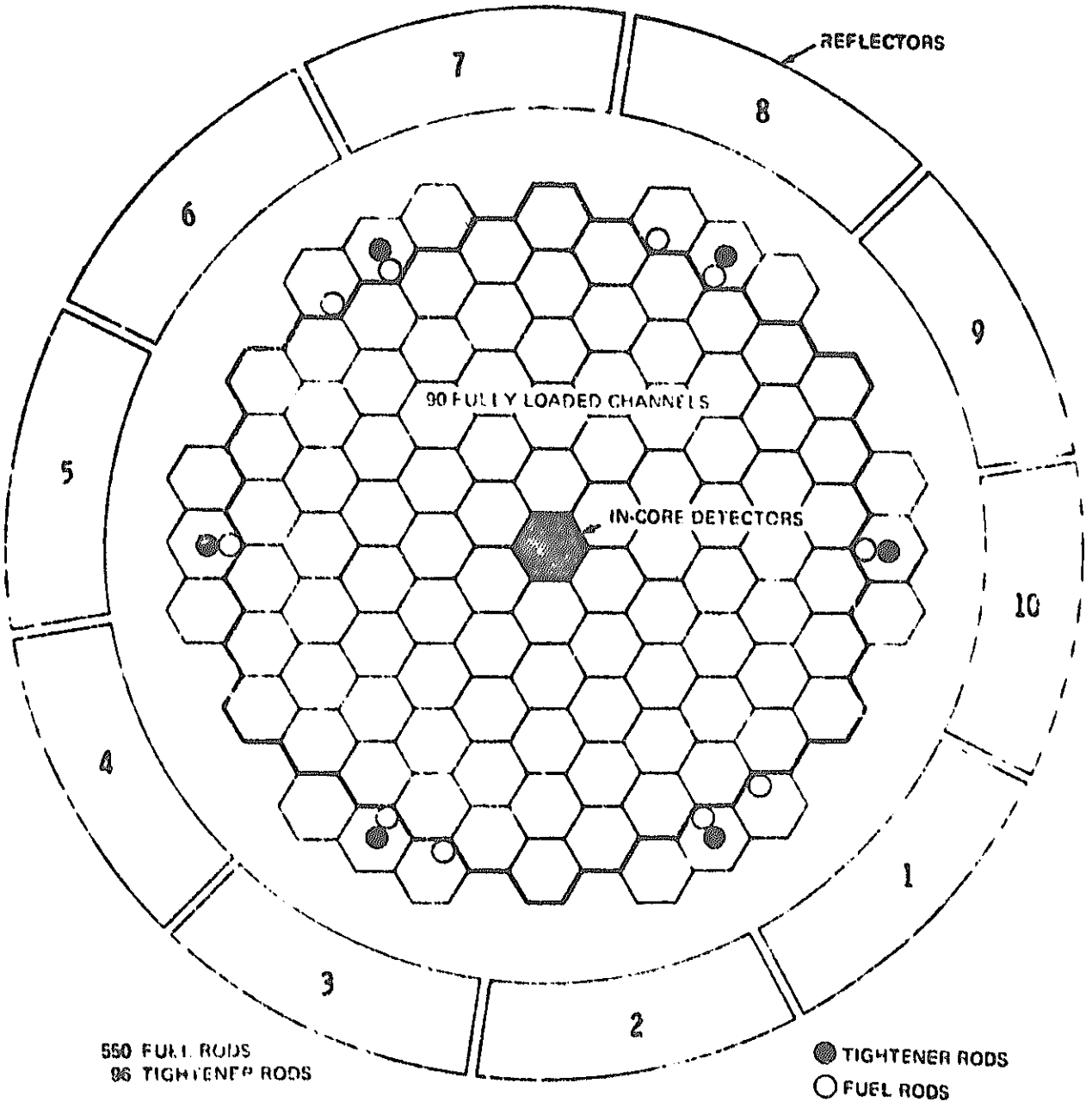

Figure 1. Assembly I-A

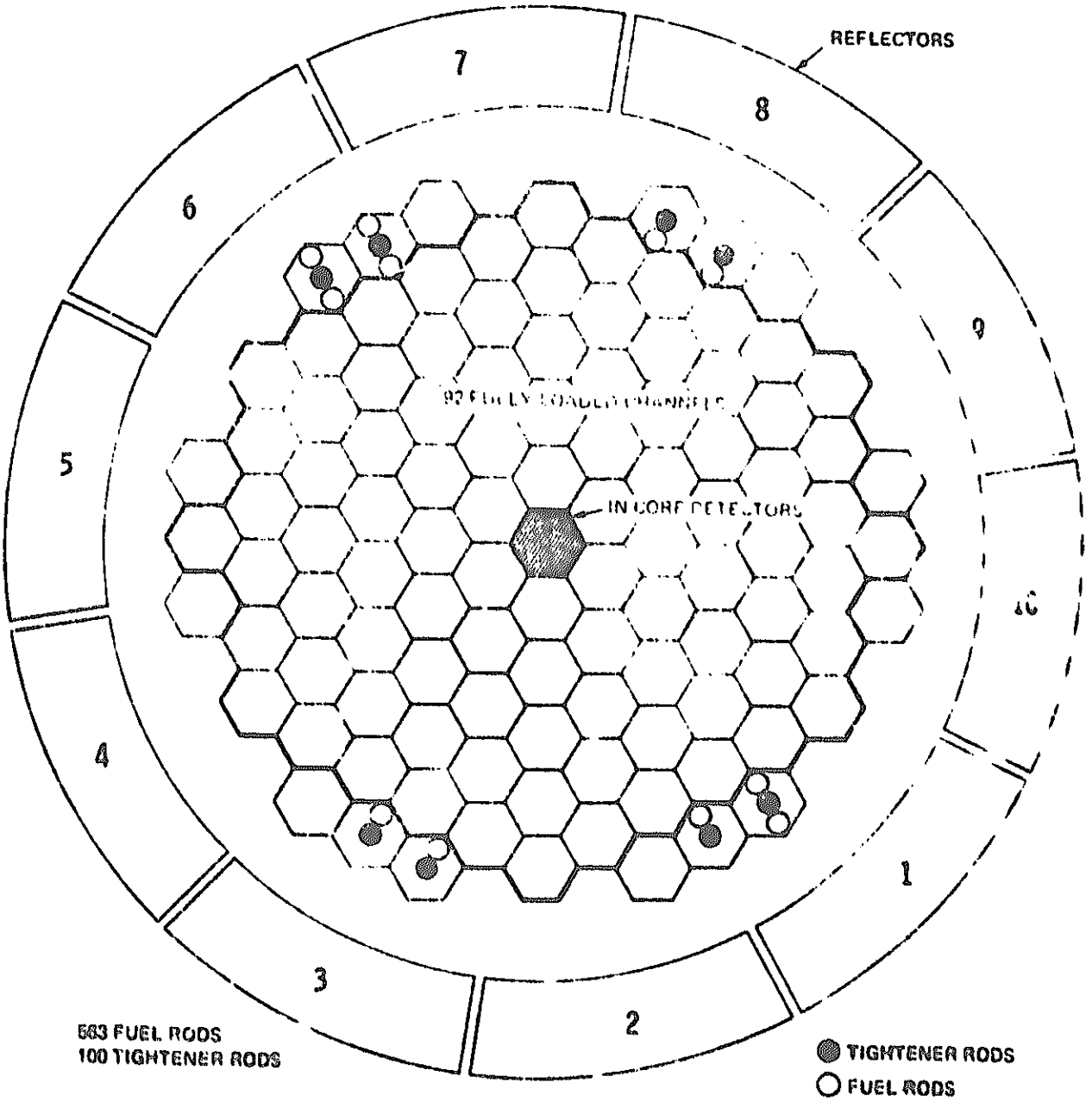

Figure 2. Assembly I-B

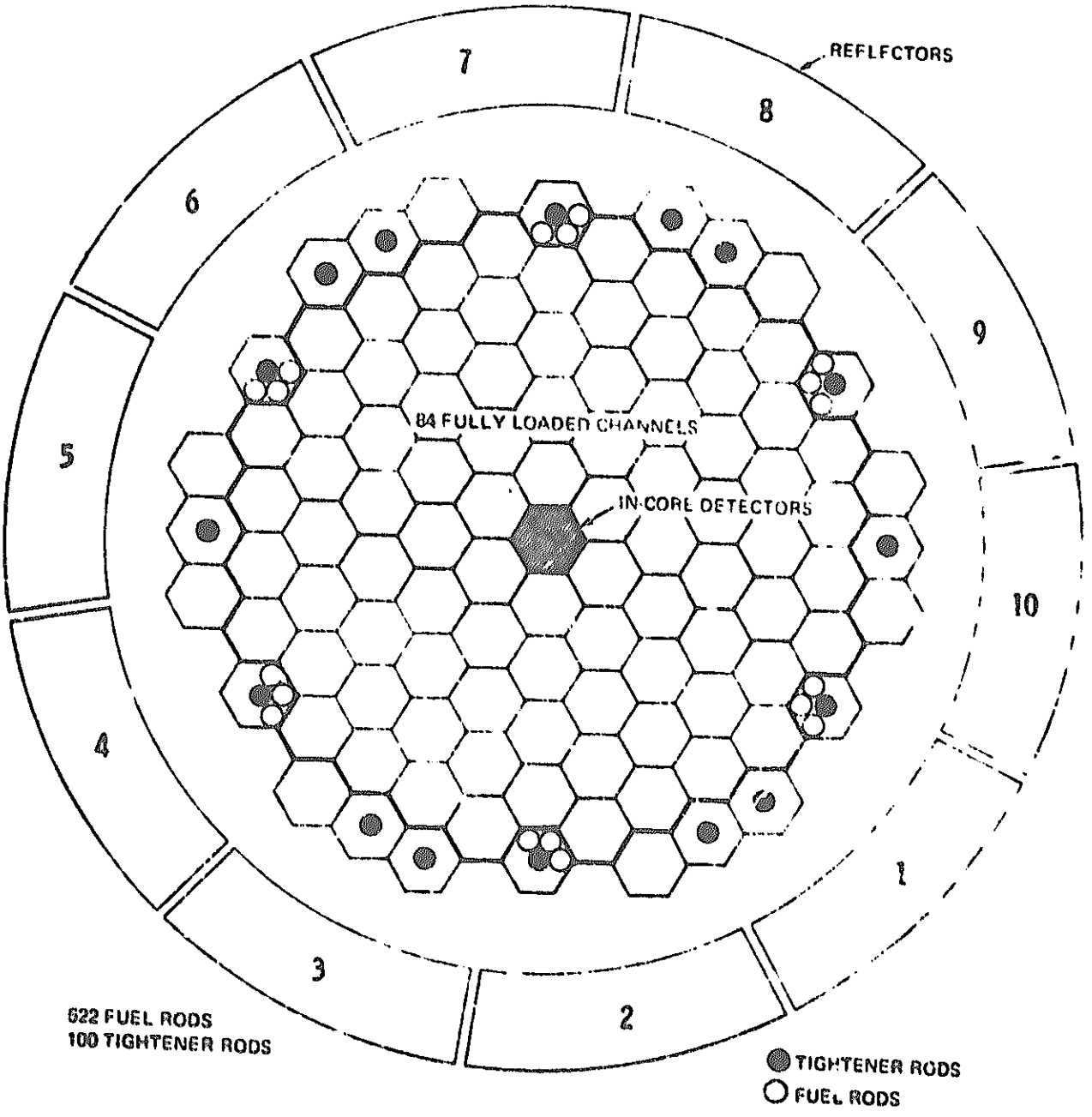

Figure 3. Assembly I-C

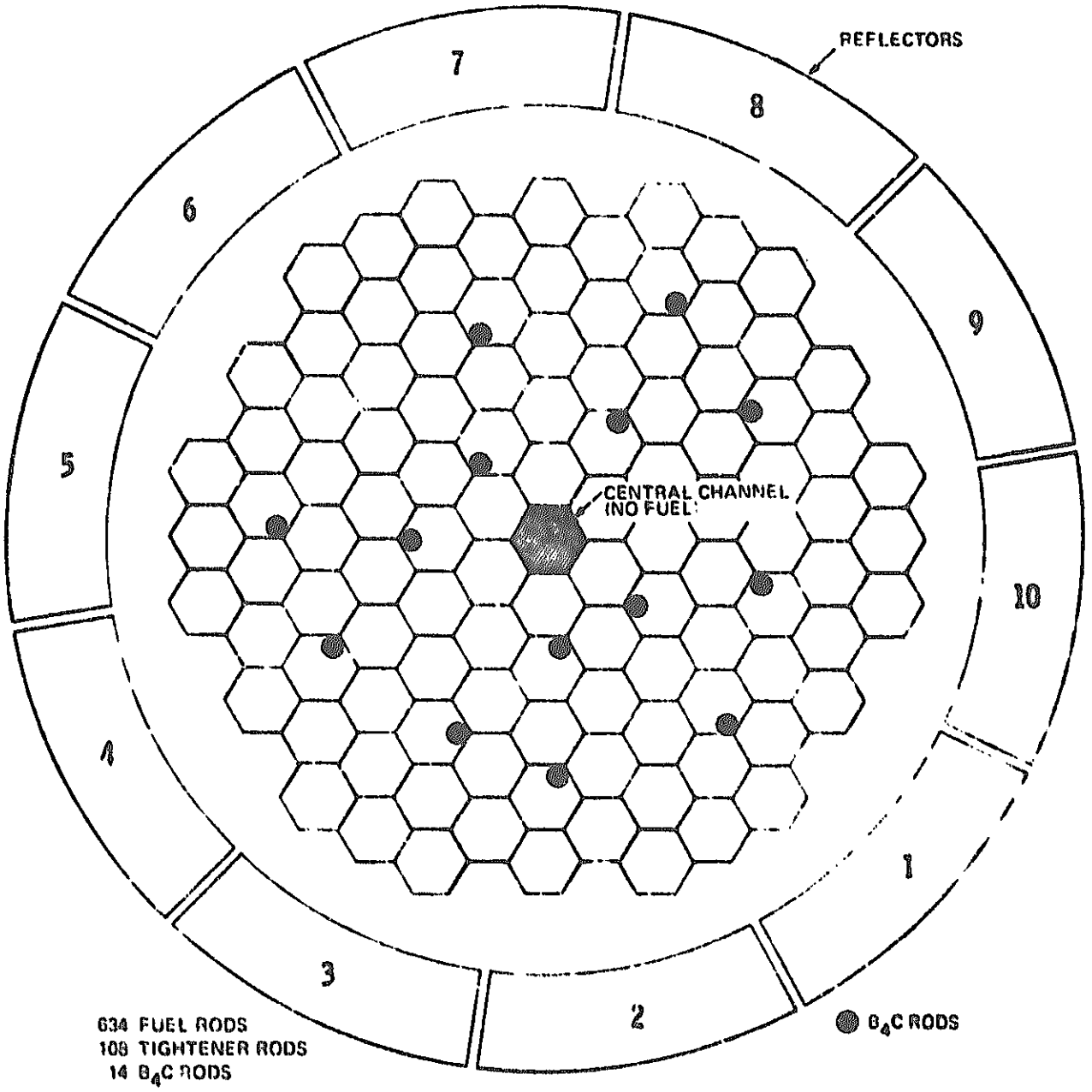

Figure 4. Assembly I-D

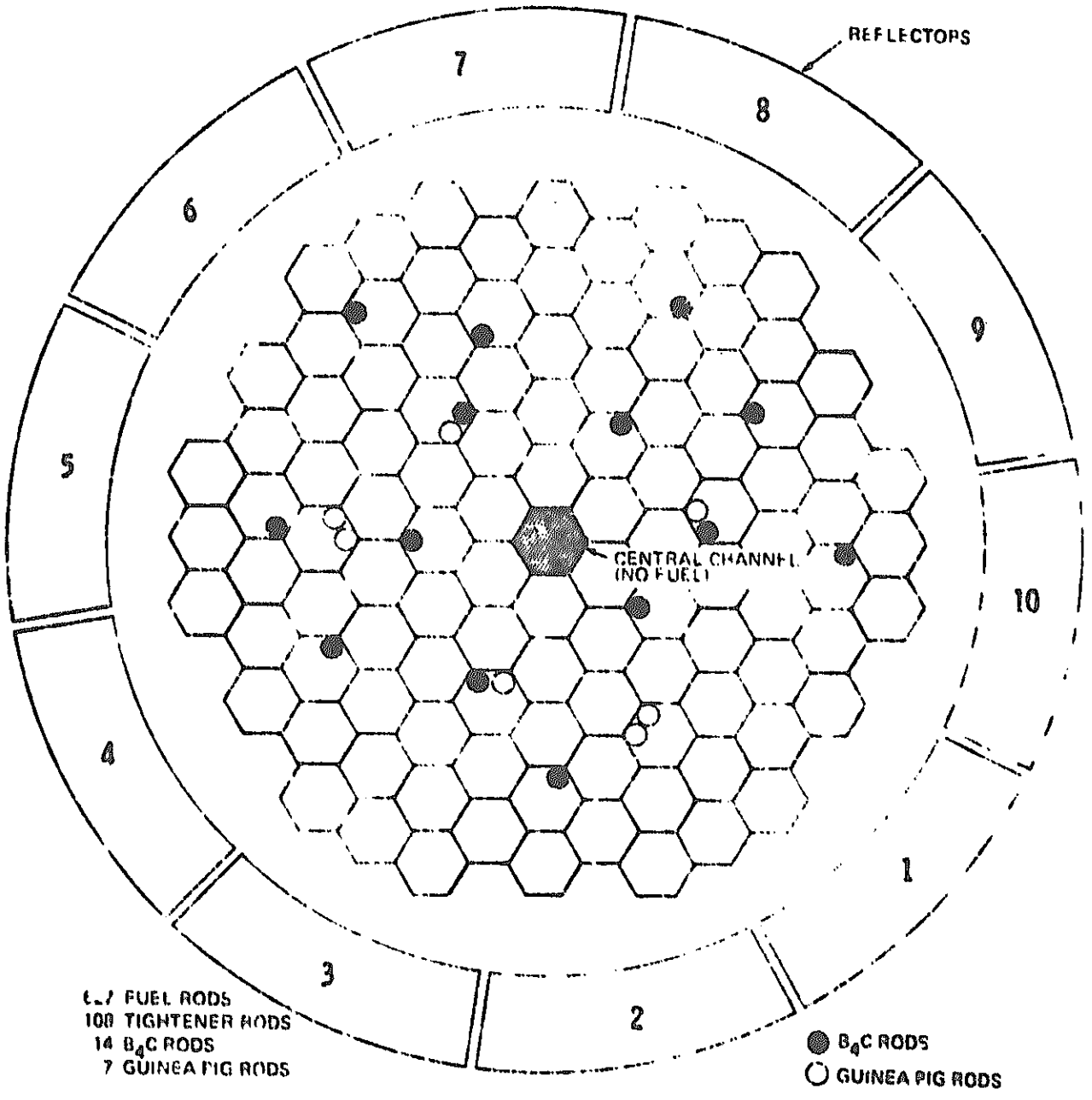

Figure 5. Assembly I-E

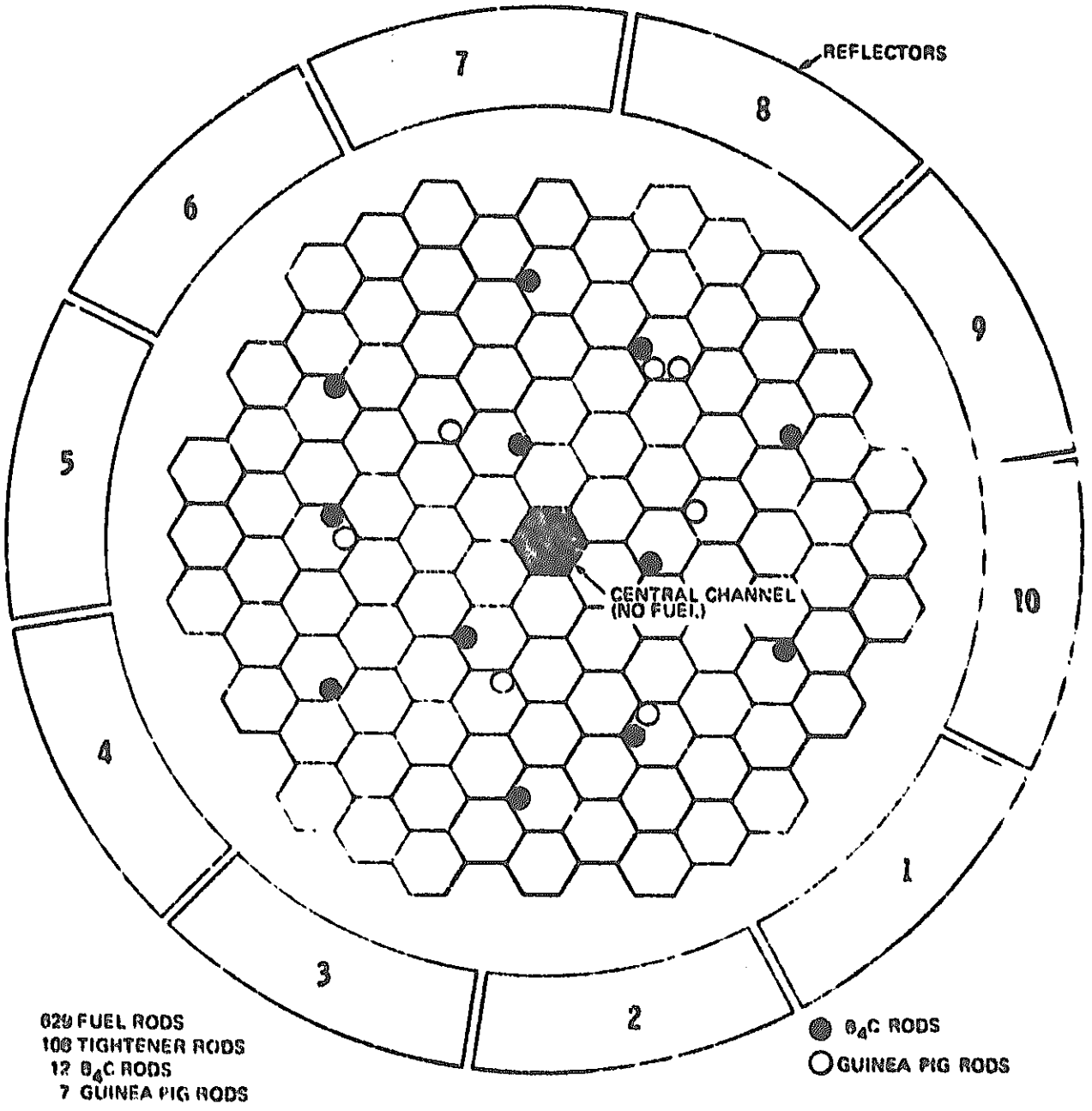

Figure 6. Assembly I-F

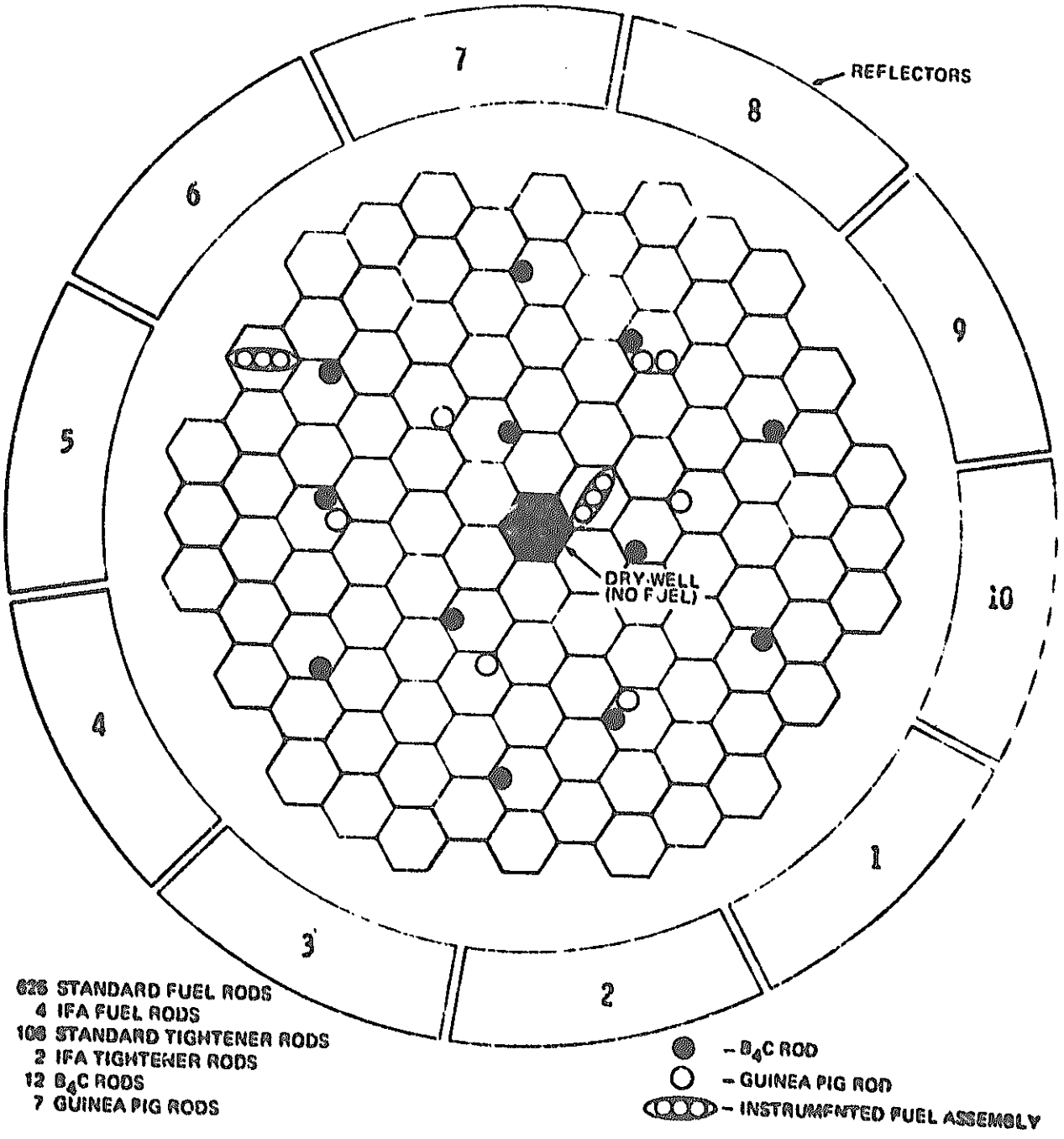

Figure 7. Assembly I-I

Purpose and Construction of Each Assembly and Measurement Made:

Table 1. Assembly Constructions, their Purposes and Measurements

Assy	Purpose and Construction	Measurements Made
I-A	The first critical loading which contained 550 fuel rods, 96 BeO tightener rods and no B_4C rods	Criticality Inherent Neutron Source Strength
I-B	13 fuel rods and 4 BeO tightener rods were added on the core periphery to provide enough excess reactivity for calibration of the reflectors	Criticality Reflector Calibration Fuel Rod Worth B_4C Rod Worth Stainless Steel Rod Worth
I-C	The low worth rods in Assy I-B were removed and replaced with fuel rods from the core periphery. A minimum critical loading of 522 fuel rods and 100 BeO tightener rods was attained	Criticality Minimum Critical Mass
I-D	Some of the fuel rods in Assy I-C were moved to the core periphery and the B_4C rods, as well as additional fuel rods and BeO tightener rods were added to the core to completely fill the 108 fuel channels	Criticality Control Rod Calibration Material Worth Reactor Noise Inherent Neutron Source Strength Fission Rate Distribution Temperature Dependent Feedback between 350°F and 400°F
I-E	In order to provide enough excess reactivity to compensate the expected reactivity feedback upon heating reactor to 760°F, and to accommodate the loading of guinea pig rods which contain 33% more Pu than a standard fuel rod, fuel and B_4C rod distribution within the core was changed	Criticality Reflector Calibration at two different temperatures (i.e. with two different critical reflector configurations for the same core loading) Flow Coefficient of Reactivity Pressure Coefficient of Reactivity Reactivity Temperature Effect between 350°F and 760°F

2 - SEFOR-1 (cont'd)

Table (cont'd)

I-F	A symmetrical loading of B_4C and guinea pig rods was arranged within the core to provide enough excess reactivity for the approach to full power operation	Criticality Fine Reflector Calibration
I-I	A final core loading was obtained by removing two standard fuel rods and one tightener rod from each of two different fuel channels in Assy I-F and replacing them with instrumented fuel assemblies (IFA's). Each IFA, which contains two temperature instrumented fuel rods and a central tightener rod, as well as sodium temperature thermocouple and a flow meter, are described in detail in reference 4.	A portion of the reactivity flow coefficient
I-J	After initial operation at 10 MW, the core loading was changed to provide additional reactivity to offset the reactivity feedback introduced by operation at higher power levels. The change in loading was made by replacing a B_4C rod in core location W3.0-S2.0E with a stainless steel rod.	Criticality Reflector Temperature Coefficient Fuel Temperature

Fuel Rod Arrangement:

See Figures 2 and 3 in 1 - SEFOR-1 (previous section).

Criticality Data:

Criticality data tabulated below are obtained at sodium temperature 350°F.

Table 2. Criticality Data

Assy	No. of Fuel rods	No. of GPR	No. of BeO rods	No. of B_4C rods	No. of IFA_f	No. of IFA_t	k_{ex} ($)
I-A	550	0	96	0	0	0	0.095
I-B	563	0	100	0	0	0	1.35
I-C	522	0	100	0	0	0	0.009
I-D	634	0	108	14	0	0	1.8
I-E	627	7	108	14	0	0	3.4
I-F	629	7	108	12	0	0	
I-I	625	7	106	12	4	2	0.2196
I-J*	625	7	106	11	4	2	0.5806

* Instead of a B_4C rod a stainless steel rod was inserted

Notes: Effective β value for reactivity scale conversion, kinetic parameters for which were taken from Keepin[8]: 0.003148
Inherent neutron source strength: less than 0.1¢ at 320 watts

Atomic Compositions:

See Table.

Additional Informations:

Measurements Made:

Criticality	(2-SEFOR)
Inherent Neutron Source Strength	(2-SEFOR)
Reflector Calibration	(see Reference 1)
Spatial Variation of Reactivity Worth	(4.1-SEFOR)

2 - SEFOR-1 (Cont'd)

Central Reaction Rates	(5.1-SEFOR)
Spatial Variation of Reaction Rates	(5.2-SEFOR)
Temperature Coefficients	(8-SEFOR)
Doppler Coefficients	(7-SEFOR)
Other Reactivities	(9-SEFOR)
Time Constant at Delayed Critical	(see Reference 1)

Related Assembly:

ZPR-3, Assembly 47

2 - SEFOR-1 (cont'd)

Theoretical Analysis:

1. Calculational Model

Fig. 8 shows a calculational model for the full core loading. The radial dimensions of the core were chosen to yield right circular cylinders of volumes equal to those of the various core regions. The homogenized composition of the various rods which were inserted into the core from time to time are summarized in Table 3 and the compositions of the unit cells and the over-all reactor model are given in Table 4 and 5. The material densities correspnding to this reactor model are given in Table 6. In other critical loadings, except full core, the outer radial region of the core contains only sodium and the steel from the channels and side rods, and from the tightener sleeve. A homogenized composition for this region is readily obtained from Table 5 by replacing all fuel, BeO and SS-316 in Composition 1 with sodium. The height of this region is the same as that of a fuel rod.

Most of the calculations were performed with either 4 or 13 energy groups. These group structures are shown in Table 7. The group cross sections were obtained from a condensation of 60 group one dimensional diffusion calculations. The source of the cross sections was the ENDF/B file, Version 1, with the exception of modifications to the fuel cross sections.

Self-shielding calculations for the fuel isotopes were performed in the 60 group structure using a cross section fitting routine with a Bell[9] approximation for resonance heterogeneity. In addition, the cross sections for nickel in the radial reflector zones were self-shielded using tables in Bondarenko and factors generated with the ENDRUN code[11].

Representative experimental and calculational results are summarized in Table 8. Agreement between experiment and calculation is generally good.

2. Prediction of Minimum Critical Size

The calculated results are shown in Table 9. The computatational methods which were used included two dimensional diffusion theory calculations[3] (2D) with 4 and 13 energy groups and two-dimensional synthesis calculations (BISYN)[10] that combined one-dimensional flux and adjoint solutions performed along the orthogonal coordinates. The results of the 2D and synthesis calculation are compared in Table 10. These multiplication factors listed in the Table include the corrections of Table 11. The 13-group 2-dimensional synthesis consistently gave about a 0.01 lower multiplication factor than the 13-group 2D calculation. Because

of this consistency, the 13-group synthesis results can be used to obtain k-values of Table 9 for which 2D calculation had not been performed.

The uncertainty of the predicted k_{eff} is ± 0.017 in reactivity.

For the detailed discussion of the correction factor in Table 11, see Reference 1.

2 - SEFOR-1 (cont'd)

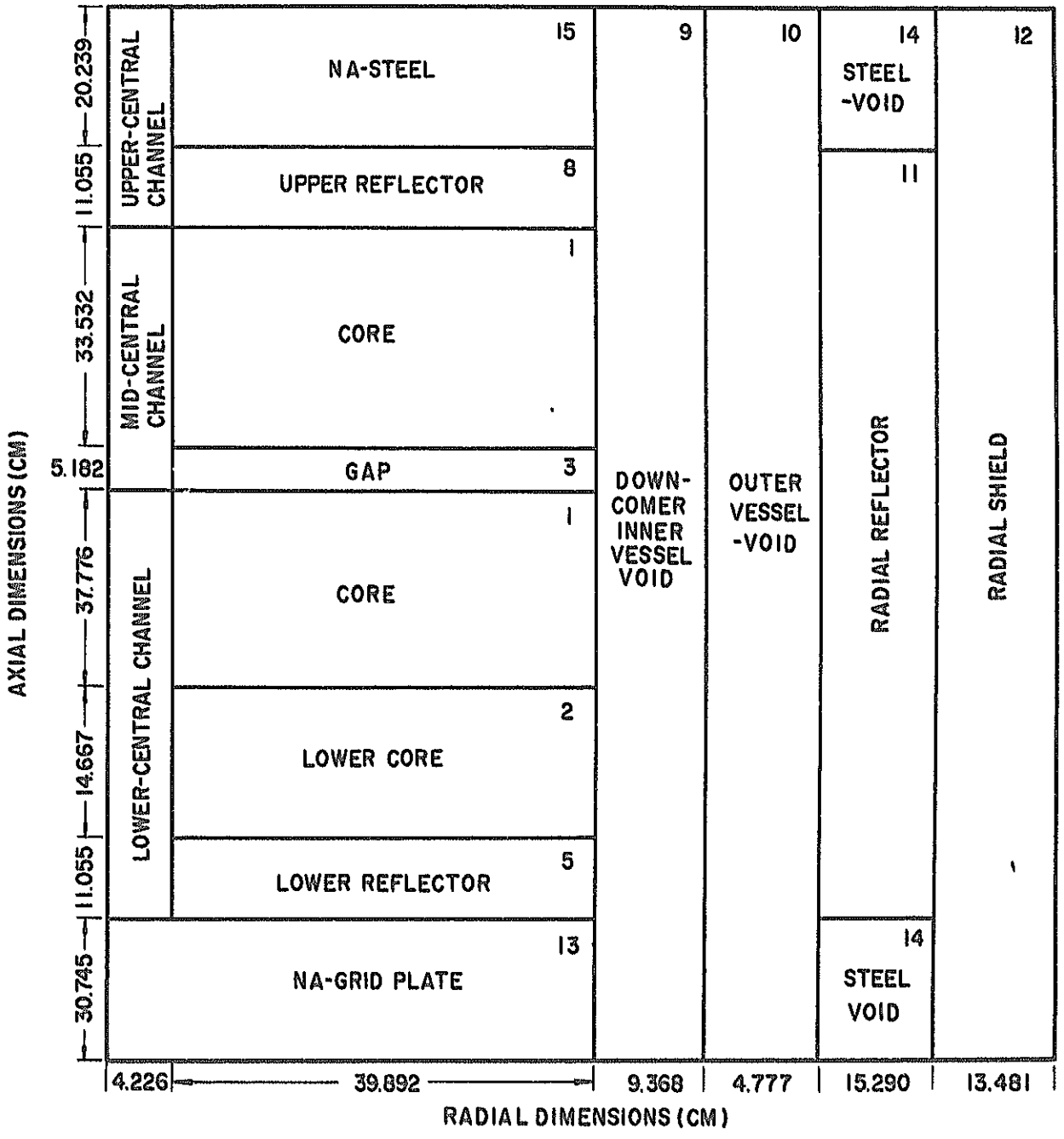

Figure 8. SEFOR Full Core Geometry (350°F)

TABLE 3

ROD COMPOSITIONS

Material	Material Volume Fractions in the Core Region of the Reactor					
	Fuel[1] and Guinea Pig[1] Rod	Tightener Rods[4] Upper Portion of Core	Tightener Rods[4] Lower Portion of Core	Core Poison Rod	Stainless Steel Rod	UO_2 Rod
Fuel[1]	0.8384[2]	-	-	-	-	-
UO_2	-	-	-	-	-	0.8384
Cladding (SS-316)	0.1616	0.1745	0.3229[3]	0.1616	0.1616	0.1616
BeO	-	0.8255	0.5868	-	-	-
SS-304 (in Steel Rod)	-	-	-	0.4982	0.8103	-
Void	-	-	0.0903	-	0.0281	-
Central Shaft (SS-304) inside Poison Rod	-	-	-	0.3402	-	-

(1) (Pu-239 + Pu-241)/(U + Pu) = $\begin{cases} 0.187 \text{ for standard fuel rods} \\ 0.250 \text{ for guinea pig rods} \end{cases}$, Pu-240/Pu = 0.0824

(2) Exclusive of gap regions where the fuel is replaced by a smeared composition of 37.5% UO_2, 3.1% inconel, 15.1% SS-304, and 44.3% void.

(3) Includes additional SS-316 inside the cladding.

(4) In the special tightener rods used for material reactivity worth measurements the BeO and boid was replaced with SS-304 at a smeared density of 7 g/cc.

Table 3 (Continued)

ROD COMPOSITIONS

Material	Material Volume Fractions in the Axial Reflector Regions of the Reactor						
	Fuel[1] and Guinea Pig[1] Rods	Tightener Rod		Core Poison Rod		Stainless Steel Rod	UO_2 Rod
		Upper Reflector	Lower Reflector	Upper Reflector	Lower Reflector		
UO_2	0.0725	-	-	-	-	-	0.0725
Ni	0.7659	0.4223	0.4730	0.8128	0.7897	-	0.7659
SS-316	0.1616	0.1609	0.1873	0.1616	0.1616	0.1616	0.1616
BeO	-	0.0710	0.0507	-	-	-	-
Void	-	0.3458	0.2890	-	0.0487	0.0281	-
Central Shaft (SS-304) inside Poison Rod	-	-	-	0.0256	-	-	-
SS-304 (in Steel Rod)	-	-	-	-	-	0.8103	-

(1) (Pu-239 + Pu-241)/(U + Pu) = $\begin{cases} 0.187 \text{ for standard fuel rods} \\ 0.250 \text{ for guinea pig rods} \end{cases}$, Pu-240/Pu = 0.0824

TABLE 4

UNIT CELL COMPOSITION

Composition	Cell Volume Fraction		
	Standard Core Unit Cell	Unit Cell in lower portion of Core	Gap Region in Core
Fuel / UO_2	0.4316	0.4316	0.1619
BeO	0.0574	0.0408	0.0574
Fuel Clad (SS-316)	0.0832	0.0832	0.0832
BeO Clad (SS-316)	0.0121	0.0224*	0.0121
Tightener Sleeve (SS-304)	0.0178	0.0178	0.0178
Channel and Side Rods (SS-304)	0.1133	0.1133	0.1784**
Sodium	0.2846	0.2846	0.2846
Inconel	-	-	0.0133
Void	-	0.0063	0.1913

* Includes extra cladding around BeO

** Includes extra SS-304 in the gap portion of six fuel rods.

TABLE 5

SEFOR FULL-CORE (648 FUEL ROD) VOLUME FRACTIONS

Volume Fraction by Region

Composition	1	2	3	4	5	6	7	8
Fuel	0.4316	0.4316	-	-	-	-	-	-
UO_2	-	-	0.1619	-	0.0373	-	-	0.0373
SS-316	0.0953	0.1056	0.0953	-	0.0962	-	-	0.0944
SS-304	0.1311	0.1311	0.1962	0.3056	0.1215	0.1177	0.1812	0.1383
Inconel	-	-	0.0133	-	-	-	-	-
BeO	0.0574	0.0408	0.0574	-	0.0035	-	-	0.0049
Sodium	0.2846	0.2846	0.2846	0.6944	0.2908	0.6944	0.6944	0.2871
Ni (Fuel Rod)	-	-	-	-	0.3943	-	-	0.3943
Ni (Tightener Rod)	-	-	-	-	0.0330	-	-	0.0294
Void	-	0.0063	0.1913	-	0.0236	0.1879	0.1244	0.0145

TABLE 5 (Continued)

SEFOR FULL-CORE (648 FUEL ROD) VOLUME FRACTIONS

Volume Fraction by Region

Composition	9	10	11	12	13	14	15
SS-316	-	-	-	-	-	-	-
SS-304	0.2855	0.1563	0.0338	0.12	0.244	0.150	0.325
Inconel	0.0202	-	-	-	-	-	-
Sodium	0.6203	-	-	-	0.706	-	0.565
Ni	-	-	0.8078	-	-	-	-
Void	0.0740	0.6461	0.1227	0.36	-	0.850	0.110
Al-Mg	-	0.1976	0.0357	0.13	-	-	-
B_4C	-	-	-	0.39	0.050	-	-

TABLE 6

SEFOR MATERIAL DENSITIES @ 350°F

Material	Density* (g/cc)
Fuel - Pu - U Oxide Oxygen/metal = 1.99 (Pu-239 + Pu-241)/(Pu+U) = 0.1870 Pu-240/Pu = 0.0824 U-235/U = 0.0022	9.587
Uranium in insulator pellets and special UO_2 rod (Oxygen/metal = 2.01)	9.786
Stainless Steel 316 and 304	7.961
Inconel	8.288
BeO	2.731
Na	0.9131
B_4C in special poison core rod B-10/B = 0.199	1.415
B_4C in radial shield	1.600
Ni in radial reflector	8.833
Ni in axial reflector	8.433
Al-Mg (96% Al, 4% Mg)	2.669

* Some of these densities are "smeared" to include void regions and should be used only with the volume fractions indicated in Tables 3 through 5.

TABLE 7

SEFOR THIRTEEN AND FOUR GROUP STRUCTURE

13 Group Structure

Group Number	Lethargy Interval	Lower Energy of Group
1	1.500	2.23 MeV
2	1.000	0.821 MeV
3	0.500	0.498 MeV
4	0.500	0.302 MeV
5	0.500	0.183 MeV
6	0.600	0.101 MeV
7	0.800	45.2 KeV
8	1.100	15.0 KeV
9	1.333	3.96 KeV
10	1.367	1.01 KeV
11	1.167	315 eV
12	1.233	91.7 eV
13	-	thermal

4 Group Structure

Group Number	Lethargy Interval	Lower Energy of Group
1	3.000	0.498 MeV
2	1.300	0.136 MeV
3	2.533	10.8 KeV
4	-	thermal

TABLE 8

REPRESENTATIVE ZERO POWER TEST RESULTS

Experiment	Measured	Calculated
Minimum Critical Core Size (Mass of Pu-239 + Pu-241)	284.3 Kg	284.9 Kg
Reflector Control Strength	9.7$	11.2$
Ratio (ℓ/β) of neutron lifetim to effective delayed neutron fraction.	2.0×10^{-4}sec	1.8×10^{-4}sec
Fuel Rod Worth near core center	+35¢	+40¢
B_4C Rod Worth near core center	-71¢	-82¢
Fission Ratios near core center		
$\sigma_f^{238}/\sigma_f^{235}$	0.0252	0.0256
$\sigma_f^{239}/\sigma_f^{235}$	0.905	0.894
Flow and pressure coefficients of reactivity	0	0
Uniform Temperature coefficient of reactivity in the following temperature ranges		
350°F to 450°F	-0.67¢/°F	-0.66¢/°F*
450°F to 550°F	-0.64¢/°F	-0.63¢/°F*
550°F to 650°F	-0.60¢/°F	-0.61¢/°F*
650°F to 760°F	-0.57¢/°F	-0.58¢/°F*

* The calculated total non Doppler effect is a constant -0.36¢/°F throughout this temperature range.

TABLE 9

CALCULATED K FOR SEFOR AND ZPR-3 ASSEMBLY 47 MOCKUPS

Reactor Model	Calculated k[d]	Normalized k[a]
ZPR-3, 1 Segment	0.995	1.005
ZPR-3, 2 Segment	0.985	0.995
SEFOR, 419 Fuel Rods	0.941	0.951
SEFOR, 464 Fuel Rods	0.966	0.976
SEFOR, 512 Fuel Rods	0.988	0.998
SEFOR, 519 Fuel Rods[b]	---	1.000[b]
SEFOR, 541 Fuel Rods[c]	1.000[c]	---
SEFOR, 554 Fuel Rods	1.006	1.016
SEFOR, 600 Fuel Rods	1.022	1.032
SEFOR, 648 Fuel Rods (Full Core)	1.038	1.048

(a). 0.01 added to calculated k values to make the average k of the ZPR-3 assembly 47 mockups equal to unity.

(b). SEFOR minimum critical core size predicted by interpolation.

(c). Minimum critical size that would have been predicted without normalization to the ZPR-3 Assembly 47 mockups.

(d). The correction factors of Table 11 are included.

TABLE 10

RESULTS OF SYNTHESIS AND DIFFUSION THEORY CALCULATIONS

Reactor Model	2-Dimensional Diffusion[b]		2-Dimensional[b] synthesis	Normalized k[a,b]
	4 Groups	13 Groups	13 Groups	
ZPR-III, 1 Segment	.989	.995	.985	1.005
ZPR-III, 2 Segment	.981	.984	.976	.995
SEFOR, 419 Fuel Rods	-	-	.931	.951
SEFOR, 464 Fuel Rods	-	-	.956	.976
SEFOR, 512 Fuel Rods	.988	-	.978	.998
SEFOR, 554 Fuel Rods	-	-	.996	1.016
SEFOR, 600 Fuel Rods	-	-	1.012	1.032
SEFOR, 648 Fuel Rods	-	1.039	1.028	1.048

(a) Normalized so that the average of the multiplication factors for the one and two segment ZPR-3 Assembly 47 mockups is equal to unity.

(b) The correction factors listed in Table 11 are included.

TABLE 11

CORRECTIONS TO DIFFUSION THEORY CALCULATIONS

	Correction Factor	ZPR-III 1-Segment	ZPR-III 2-Segment	SEFOR 512 Rods	SEFOR 648 Rods
a)	Transport Core Leakage Effect	+0.0086	+0.0089	+0.0097	+0.0089
b)	Cell Heterogeneity				
	High Energy	+0.0067	+0.0067	+0.0042	+0.0042
	Low Energy	-0.0017	-0.0017	-0.0004	-0.0004
	Leakage	-0.002	-0.002	-0.001	-0.001
c)	Excess Reactivity in ZPR-III Mockup Models	-0.0073	-0.0042	-	-
d)	Non-cylindrical Outer Periphery	-	-	-0.003	-0.003
e)	Doppler Effect (80 → 350°F)	-	-	-0.003	-0.0033
f)	Overshielding Nickel Reflector	+0.001	+0.001	+0.001	+0.001
	Total Correction	+0.0053	+0.0087	+0.0075	+0.0064

References:

1. L.D. Noble et al., GEAP-13588 (March, 1970) pp.4-8

2. R.A. Meyer et al., GEAP-13598 (June, 1970) Section II

3. R. Protsik and G.E. Leff, GEAP-13537 (Sept., 1969)

4. E.R. Craig, GEAP-5615 (April, 1968)

5. GEAP-5754 (Nov. 1968 - Jan., 1969) pp.35-40

6. GEAP-10010-20 (Feb. - April, 1969) pp.9-11

7. GEAP-10010-26 (Aug. - Oct., 1970) pp.15-16

8. G.R. Keepin, "Physics of Nuclear Kinetics", Addison-Wesley, 1965

9. G.I. Bell, N.S.E. 5 p.138 (1959)

10. P. Greebler et al., GEAP-4922 (July, 1965)

11. B.A. Hutchins, G.E. - BRDO memo, (June, 1968)

4.2 - SEFOR-1 Spatial Variation of Reactivity Worth

Facility: SEFOR Assembly: I

A. Experiment in Assembly I-B

Experimental Method:

The reactivity worths of fuel (18.7% fissile Pu), B_4C and stainless steel rod were measured at four different radial core locations in the 563 rod partially loaded core Assembly I-B. In addition, the reactivity worths of four BeO tightener rods on the core periphery were measured. The reactivity worths of fuel, B_4C and stainless steel rods at a given location were measured by recording the reactor temperature and the critical reflector positions with the following core arrangements; the core loading with the original fuel rod in place; the original fuel rod removed - the fuel rod location thus being filled with liquid sodium; the original fuel rod replaced by the reference fuel rod, the B_4C rod, or the stainless steel rod; and finally the core with the original rod re-inserted. The worth of the peripheral BeO tightener rod in Assembly I-B was determined from the critical reflector configurations occurring before and after insertion of four rods into sodium filled tightener rod locations. The position within the core at which measurements were made are illustrated in Fig 1.

Results:

The results are tabulated in Table 1 along with the calculated values.

During the measurements a fuel rod that was substantially low (approximately 40%) in worth was found and an extensive investigation was undertaken to determine the extent of the problem. The investigation showed that a number of rods were low in worth. The very low worth rods were removed after completion of the experiments on Assembly I-B.

Precision:

Based on critical check measurements, the estimated standard deviation in a single measurement of a small reactivity change, calculated from the difference between two measurements of the critical point, is 0.37 $\sqrt{2}$ cents, or 0.5 cents. The calibration uncertainty in any reactivity change of magnitude Δk cent would be expected to be approximately 0.08 $\sqrt{\Delta k/9}$ cents, and the total un-

certainty in any reactivity would thus be $[2(0.37)^2+(0.08)^2\Delta k/9]^{1/2}$. This relation is probably reasonable for reactivity changes which are of order of 30 cents or less. Detailed descriptions are given in Ref. 1.

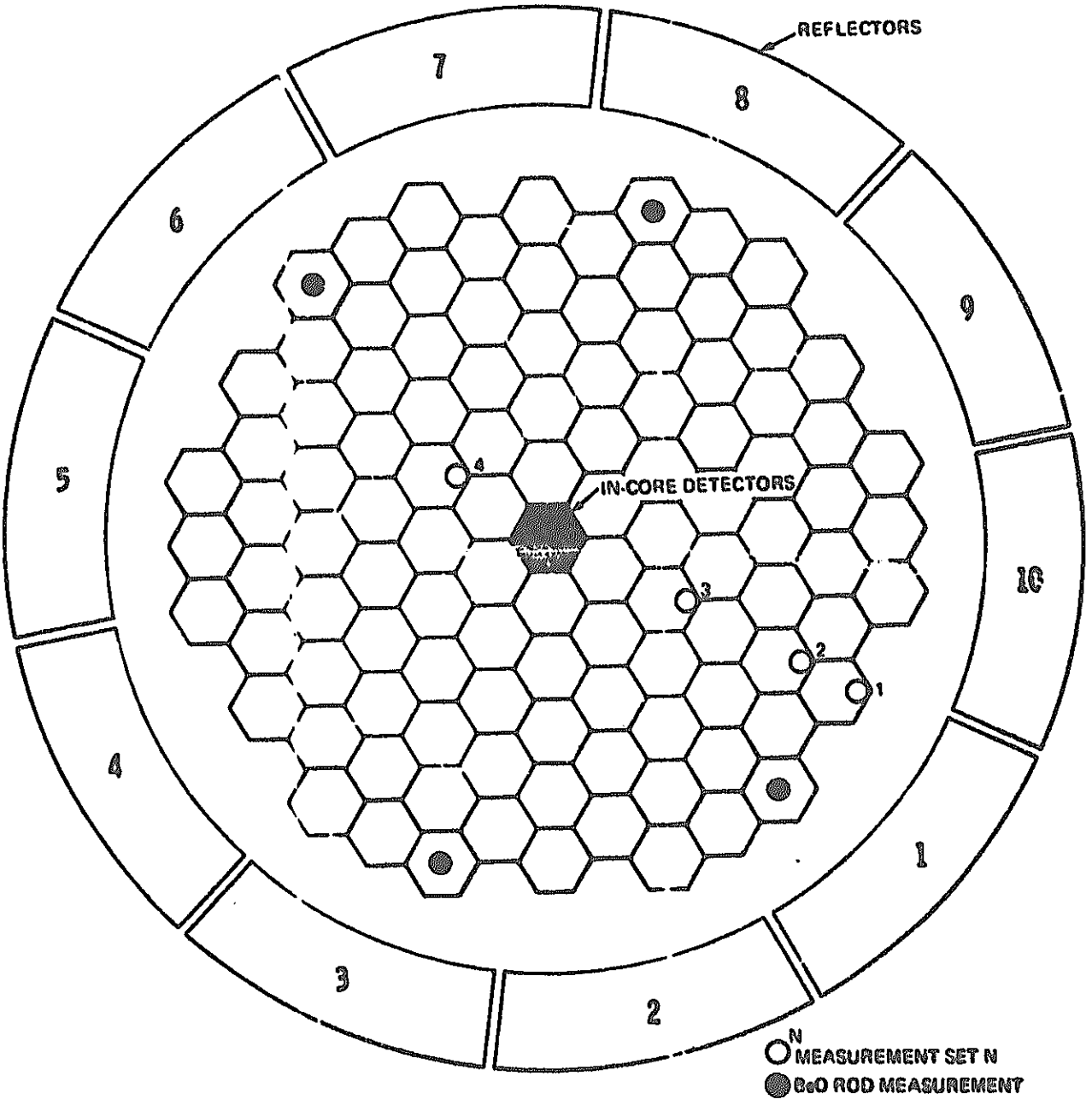

Figure 1. Location of Material Worth Measurements in Assembly 1-B

TABLE 1

MATERIAL REACTIVITY WORTH MEASUREMENTS

(ASSEMBLY I-B)

Measurement Set Number	Core Location*	Type of Rod	Worth Relative to Sodium (cents) Measured**	Calculated*** (β=0.00323)
1	W2.5-S5.0-B (Radius=42.7cm)	Fuel (No. 414)	+ 8.1	+ 8.8
		Fuel (No. 781)	+ 8.4	+ 8.8
		Stainless Steel	+ 1.7	--
		B_4C	-14.3	-14.9
2	W2.0-S4.0-B (Radius=34.6cm)	Fuel (No. 635)	+15.3	+16.6
		Fuel (No. 781)	+15.7	+16.6
		Stainless Steel	+ 1.7	+ 2.5
		B_4C	-23.7	-23.0
3	W1.0-S2.0-B (Radius=18.6cm)	Fuel (No. 874)	+17.6	+37.4
		Fuel (No. 781)	+30.5	+37.4
		Stainless Steel	- 2.5	- 3.3
		B_4C	-60.7	-69.8
4	E1.0-N2.0-B (Radius=13.8cm)	Fuel (No. 791)	+40.2	+42.4
		Fuel (No. 781)	+39.3	+42.4
		Stainless Steel	- 3.9	- 4.4
		B_4C	-74.6	-83.8
	W4.0-S4.0 E4.0-N4.0 E5.0-S2.0 W5.0-N2.0 (Radius=42.6cm)	4 BeO Tightener Rods	+16.0	+16.0

* See Core loading Diagram.

** The estimated standard deviation in the measurement is approximately ±0.5 cents (see Precision).

*** Perturbation results of a two-dimensional synthesis calculation.

B. Experiment in Assembly I-D

Experimental Method:

The reactivity worths of fuel (18.7% fissile Pu), B_4C, stainless steel, guinea pig (25% fissile Pu), depleted UO_2, and BeO tightener rods were measured at several locations in Assembly I-D. The measurements were performed in the same manner as in Assembly I-B (described in Item A) with the addition that a guinea pig and a depleted UO_2 rod were substituted for the original fuel rods during the sequence of measurements. The worths of the BeO tightener rod in Assembly I-D were determined at four radial locations by replacing the original BeO rods in these locations with special stainless steel tightener rods. The position within the core at which measurements were made are illustrated in Fig. 2.

Results:

The measured worths of fuel, B_4C, UO_2, and guinea pig rods are tabulated in Tables 2 through 4 along with calculated results.

Precision:

Refer to the descriptions in Item A.

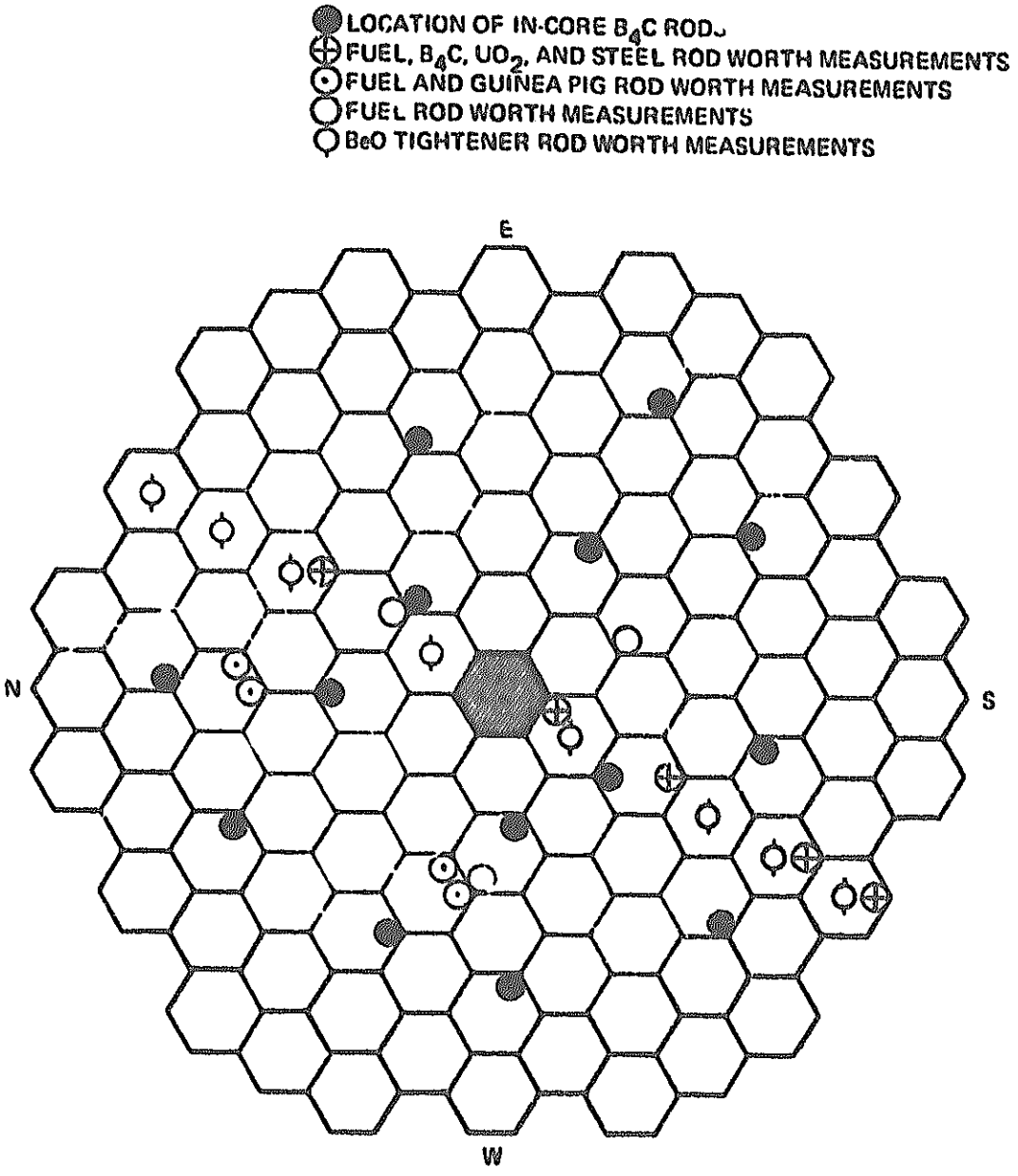

Figure 2. Locations of Material Worth Measurements in Assembly 1-D

TABLE 2

MATERIAL REACTIVITY WORTH MEASUREMENTS

(Assembly I-D)

Core Location*	Type of Rod	Worth Relative to Sodium (cents) Measured**	Calculation*** (β=0.00315)
W2.5 - S5.0-B (Radius=42.7cm)	Fuel (No. 121)	+ 8.7	+ 8.5
	Fuel (No. 781)	+ 9.2	+ 8.5
	Stainless Steel	+ 2.1	+ 0.8
	UO_2	0.0	- 1.1
	B_4C	-13.0	-17.5
W2.0 - S4.0-B (Radius=34.6cm)	Fuel (No. 635)	+14.6	+16.2
	Fuel (No. 781)	+15.4	+16.2
	Stainless Steel	- 0.4	- 1.3
	UO_2	- 2.7	- 4.6
	B_4C	-22.1	-28.5
E1.5 - N3.0-B (Radius=21.8cm)	Fuel (No. 695)	+27.8	+29.6
	Fuel (No. 781)	+27.6	+29.6
	Stainless Steel	- 1.6	- 5.0
	UO_2	- 7.6	-11.4
	B_4C	-49.1	-53.7
W1.0 - S2.0-B (Radius=18.6cm)	Fuel (No. 783)	+28.4	+32.7
	Fuel (No. 781)	+28.8	+32.7
	Stainless Steel	- 2.8	- 6.0
	UO_2	- 9.8	-12.9
	B_4C	-52.3	-59.8
W0.5 - S1.0-F (Radius=5.8cm)	Fuel (No. 781)	+34.5	+38.7
	Stainless Steel	- 3.6	- 7.3
	UO_2	-13.0	-17.2
	B_4C	-70.9	-79.0

* See Core Loading Diagram.

** The estimated standard deviation in the measurements is approximately ±0.5 cents (see Precision in Item A).

*** Perturbation Results of a one-dimensional diffusion calculation.

TABLE 3

GUINEA PIG AND ADDITIONAL FUEL ROD WORTH MEASUREMENTS

(ASSEMBLY I-D)

Core Location*	Type of Rod	Worth Relative to Sodium (cents)	
		Measurement**	Calculation*** (β=0.00315)
W0.0 - N4.0-A (Radius=26.6cm)	Fuel (No. 781)	+23.1	+24.8
	Guinea Pig (No. A04)	+33.5	+36.0
W0.0 - N4.0-B (Radius=25.1cm)	Fuel (No. 532)	+24.7	+26.3
	Fuel (No. 781)	+24.1	+26.3
	Guinea Pig (No. A04)	+35.4	+38.2
W2.5 - N1.0-B (Radius=20.6cm)	Fuel (No. 666)	+26.7	+30.9
	Fuel (No. 781)	+27.0	+30.9
	Guinea Pig (No. A04)	+39.4	+45.2
W2.5 - N1.0-A (Radius-18.6cm)	Fuel (No. 831)	+27.6	+32.7
	Fuel (No. 781)	+28.3	+32.7
	Guinea Pig (No. A04)	+41.8	+48.0
W2.0 - N0.0-D (Radius=18.6cm)	Fuel (No. 774)	+27.9	+32.7
	Fuel (No. 781)	+27.9	+32.7
E1.0 - N2.0-B	Fuel (No. 791)	+33.7	+36.3
E1.0 - S2.0-D (Radius=13.8cm)	Fuel (No. 626)	+32.7	+36.3

* See Core Loading Diagram.

** The estimated standard deviation in the measurements is approximately ±0.5 cents.

*** Perturbation results of a one-dimensional diffusion calculation.

TABLE 4

TIGHTENER ROD REACTIVITY WORTH MEASUREMENTS

(ASSEMBLY I-D)

Core Location*	Type of Rod	Worth Relative to Stainless Steel (cents) Measurement**	Calculation*** (β= 0.00315)
W2.5 - S5.0 E2.5 - N5.0 (Radius=40.3cm)	BeO BeO	4.6	5.4
W2.0 - S4.0 E2.0 - N4.0 (Radius=32.2cm)	BeO BeO	5.7	5.0
W1.5 - S3.0 E1.5 - N3.0 (Radius=24.2cm)	BeO BeO	6.1	5.2
W0.5 - S1.0 E0.5 - N1.0 (Radius=8.0cm)	BeO BeO	4.5	6.0

* See Core Loading Diagram.

** The worth of substituting two rods simultaneously. The estimated standard deviation in the measurements is ±0.5 cents.

*** Perturbation results of a one-dimensional diffusion calculation.

Theoretical Analysis:

1. Assembly I-B

The results obtained using perturbation calculations of 13 group two-dimensional synthesis solutions and the calculated effective delayed neutron fraction, β, for this assembly of 0.00323, are shown in Table 1 along with the measured results.

It is worthy of note that better agreement between the experimental and calculated values is obtained by increasing the calculated effective delayed neutron fraction β by 6%.

2. Assembly I-D

The reactivity worths were calculated from perturbations(+) of one-dimensional diffusion and two-dimensional true and synthesis calculations (Tables 2 ~ 5) and in addition, various rod worths were calculated using a reactor model in which a portion of the original fuel rods in a thin annular ring were replaced with sodium or one of the test rods. The calculational results of the latter effects at a few locations using a true two- dimensional diffusion program are compared with experiment in Table 5.

As was true with the results for Assembly I-B, better agreement between experiment and calculation would generally be obtained if the value of the calculated effective delayed neutron fraction (β = 0.00315 for Assembly 1D) were increased by 6 to 10%.

(+) Perturbation results of radial one-dimensional diffusion theory calculation are strongly influenced by the perpendicular bucklings which are used in the radial regions outside the core. For a one-dimensional calculation which provided reasonable agreement with experiment, the non-core buckling values of the one-segment mockup in ZPR-3 Assembly 47 were used. The validity of approximating the non-core buckling values of two-segment core by those of one-segment core is discussed in Reference 1.

TABLE 5

COMPARISON OF CALCULATED AND EXPERIMENTAL MATERIAL REACTIVITY WORTHS

	Worth from synthesis perturbation calculation (¢)	Worth from one-dimensional perturbation calculation (¢)	Worth from two-dimensional diffusion calculation (¢)	Experimental Worth* (¢)
Fuel Rod Worth				
radius= 9.4 cm	43.0	39.2	39.7	36.0*
radius=40.4 cm	12.0	10.5	11.7	10.5*
B_4C Rod Worth				
radius= 9.4 cm	-83.0	-74.0	-78.0	-66.5*
radius=40.4 cm	-19.5	-20.0	--	-15.5*
UO_2 Rod Worth				
radius= 9.4 cm	-16.0	-16.3	--	-12.5*
radius=40.4 cm	- 1.4	- 1.4	--	- 0.5*
Guinea Pig Rod Worth				
radius= 19 cm	50.5	47.5	--	41.5*
radius= 26 cm	39.5	37.0	--	34.5*

* The experiments were actually performed at other radii (see Tables 2 and 3). The values shown here were obtained by interpolation among the measured values.

4.2 - SEFOR-1 (cont'd)

References:

1. L.D. Noble et al., GEAP-13588 (March, 1970) pp.59 - 86.

2. GEAP-10010-21 (May - July, 1969) pp.37 - 44.

3. GEAP-10010-22 (Aug. - Oct., 1969) pp.24 - 31.

5.1 - SEFOR-1 Central Reaction Rate Ratio

Facility: SEFOR Assembly: I

Experimental Method:

A count rate data was taken on the three foils near the core center (can number 3, rod FB) to determine foil fission ratios in Assembly I-D. The 1.6 MeV La-140 fission product emission was counted for the depleted uranium, enriched uranium and plutonium foils in this can. The enriched uranium and plutonium foils were counted for one hour twenty minutes and the depleted uranium foil was counted for fifteen hours thirty seven minutes. The data was recorded on a multi-channel analyser and the area under the total energy peak of the 1.6 gamma ray was integrated for each foil.

The area under the total energy peak consists of the 1.6 MeV events from the decay of La-140 plus background from other fission products. The background was assumed to have the same shape and magnitude as the spectrum just above the 1.6 MeV peak. This background was subtracted from the area of the total energy peak and the resulting count rate was then normalized to the foil weight to obtain the specific "La-140" activity for each type of foil.

Results:

The foil fission ratios are as follows after accounting for count length, mass and yield

$$\frac{\sigma(\text{Depleted U})}{\sigma(\text{Enriched U})} = 0.0290$$

$$\frac{\sigma(\text{Pu Mixture})}{\sigma(\text{Enriched U})} = 0.9215$$

The U-238 to U-235 fission ratio is obtained directly from these values. The Pu-239 to U-235 ratio was obtained from the measured foil ratios by treating the small amount of Pu-241 as if it were Pu-239, and by treating the other isotopes as Pu-240. In addition the calculated Pu-240 to U-235 fission ratio of 0.206 was used to obtain a correction of 0.013 in the value of 0.905. The results are as follows. (Ref. 2)

$$\sigma_f^{238} / \sigma_f^{235} = 0.0252$$

$$\sigma_f^{239} / \sigma_f^{235} = 0.905$$

Precision:

No normalization was made for differences in counting time. The counts were treated as if they had been taken in the middle of the counting interval and the three count intervals were assumed to be at the same time after shutdown. The first assumption results in less than one percent error (see Ref. 5), while the second assumption results in less than 2% error.

The estimated outside error limit ($\sim 2\sigma$) on the foil fission ratios is about 10%. This limit is due to a combination of uncertainties in La-140 yield, counting statistics, background subtraction, weight normalization and counting geometry reproducibility.

5.1 - SEFOR-1 (cont'd)

Theoretical Analysis:

Cross section ratios between U-235, U-238, Pu-239, and Pu-240 have been calculated for the SEFOR full size core (I-D) and are summarized in Table 1. These ratios are essentially independent of B_4C content (e.g., all of the tabulated ratios changed by ≤1% when 7 of the 19 B_4C rods in the reference calculation were replaced by fuel rods) and should be representative of any fully-loaded SEFOR core. The cross section ratios were obtained from 13 group calculations using the BISYN computer program.

TABLE 1

CROSS SECTION RATIOS FOR THE

SEFOR FULL SIZE CORE

Ratio	Core Average Value	Value at Peak* Power Point
$\sigma_f^{238} / \sigma_f^{235}$	0.0245	0.0256
$\sigma_f^{239} / \sigma_f^{235}$	0.877	0.894
$\sigma_f^{240} / \sigma_f^{235}$	0.198	0.206
$\sigma_c^{235} / \sigma_f^{235}$	0.308	0.297
$\sigma_c^{238} / \sigma_f^{235}$	0.126	0.129
$\sigma_c^{239} / \sigma_f^{235}$	0.234	0.228
$\sigma_c^{240} / \sigma_f^{235}$	0.228	0.208

* The peak power point occurs ∿ 3-1/2 inches below the core midplane adjacent to the central channel.

5.1 - SEFOR-1 (cont'd)

References:

1. L.D. Noble et al., GEAP-13588 (March, 1970) pp.93 - 94.

2. GEAP-5576 (Jan., 1968) pp.3.10 - 3.39.

3. GEAP-10010-21 (May - July, 1969) pp.49 - 50.

4. GEAP-10010-24 (Feb. - April, 1970) pp.40 - 42.

5. W.F. Welsh, PWAC 474 (July, 1965) p.49.

5.2 - SEFOR-1 Spatial Variation of Reaction Rate

Facility: SEFOR Assembly: I

Experimental Method:

The spatial distributions of the fission rate for the isotopes Pu-239, U-238, and U-235 were measured in Assembly I-D. Foils of these isotopes were placed at selected axial positions in six special foil holder rods. These rods were inserted into the core at selected radial locations and irradiated for approximately 1 hour at a nominal reactor power of 1 kW. After removal from the core, the fission product gamma activity of each foil was obtained with a Na-I crystal scintillation counter. The energy window for the counting of all foils was the same, and covered the range between 430 and 730 keV. This region included several gamma peaks which are compositions of fission product peaks.

The specified isotopic compositions of the thin cylindrical foils are listed on table 1. The weight of the uranium foils was of the order of 120 milligrams, while that of the Al-clad foils (a Pu-Aℓ alloy of 99.01% Pu) was about 23 milligrams.

Table 1. Foil Isotopic Compositions

Foil Type	Isotopic Composition Isotope	Percent
Enriched Uranium	U-235	93.15
	U-238	6.85
Depleted Uranium	U-235	0.19
	U-238	99.81
Plutonium	Pu-238	0.036
	Pu-239	92.905
	Pu-240	6.444
	Pu-241	0.582
	Pu-242	0.033

The fissionable foils were placed in cylindrical Aℓ "cans" that were 0.27 inches in height with an outer diameter of 0.475 inches. The fissionable foils within a given can were separated from each other and from the ends of the can by Aℓ foils. The cans were positioned vertically within the special foil holder rod, by Aℓ spacers. The position of the cans and spacers within

a foils holder rod is indicated in Table 2.

The fissionable foils within a given can were separated from each other and from the ends of the can by Aℓ foils. The cans were positioned vertically within the special foil holder rod, (see Fig. 1) by Aℓ spacers. The position of the cans and spacers within a foil holder rod is indicated in Table 2. The axial position of the foils above the bottom of the core (not including the lower uranium insulator pellet) is also shown in the table. In calculating the axial foil positions, it was assumed that all foils were 0.098 inches above the bottom of the foil can.

Six of the standard fuel rods in core loading Assembly I-D were replaced by the special foil holder rods. Their location within the core is shown in Fig. 1. With this core configuration the reactor was brought critical with reflector #8 at a position of ∿47 cm relative to a completely raised position of ∿98 cm and all other reflector were completely raised.

Results:

The measured specific activities for all the foils are tabulated in Tables 3 through 5. The corrections for background gamma events in the foils, small difference in foil weight, and activity decay during the counting process are included. The background corrections for U238 and Pu239 were about 5% of the observed count rate in the irradiated foils of lowest activity. Background corrections for the U235 were negligible. The corrections for the decay of the activity were determined from the measured time dependence of the specific activity for each foil. These corrections were 3% or less for foils within the same rod but ranged up to ∿23% for foils in different rods.

Additional Information:

The power distribution obtained as a composition of these experimental values and the calculated Pu239/U238 fission ratio at the core centre is given in Ref. 2.

TABLE 2

FOIL POSITIONS IN FOIL HOLDER RODS

Position Number	Height of Al Spacers Below Can at 70°F (inches)	Can Width* at 70°F (inches)	Foil Height** above bottom of core at 350°F (cm)
1	0.75	0.27	1.2
2	9.50	0.27	26.1
3	4.00	0.27	37.0
4	6.00	0.27	53.0
5	0.50	0.27	54.9
6	1.00	0.27	58.2
7	5.75	0.27	73.5
8	6.50	0.27	90.8

* In some rods a few cans were replaced with 1/4 inch spacers.

** Foils located 0.098 inches (at 70°F) above bottom of can. The bottom of the first can is 3/8 inches above the bottom of the core. A linear expansion coefficient of 1.3×10^{-5}/°F was used for the aluminum. The core height at 350°F is 91.2 cm.

5.2 - SEFOR-1 (cont'd)

ROD	LOCATION
FB	W0.5–S1.0E
FC	W2.0–S2.0B
FD	W4.0–S4.0B
FE	E4.5 S3.0F
FF	W4.5–N3.0C
FG	W2.5–N1.0F

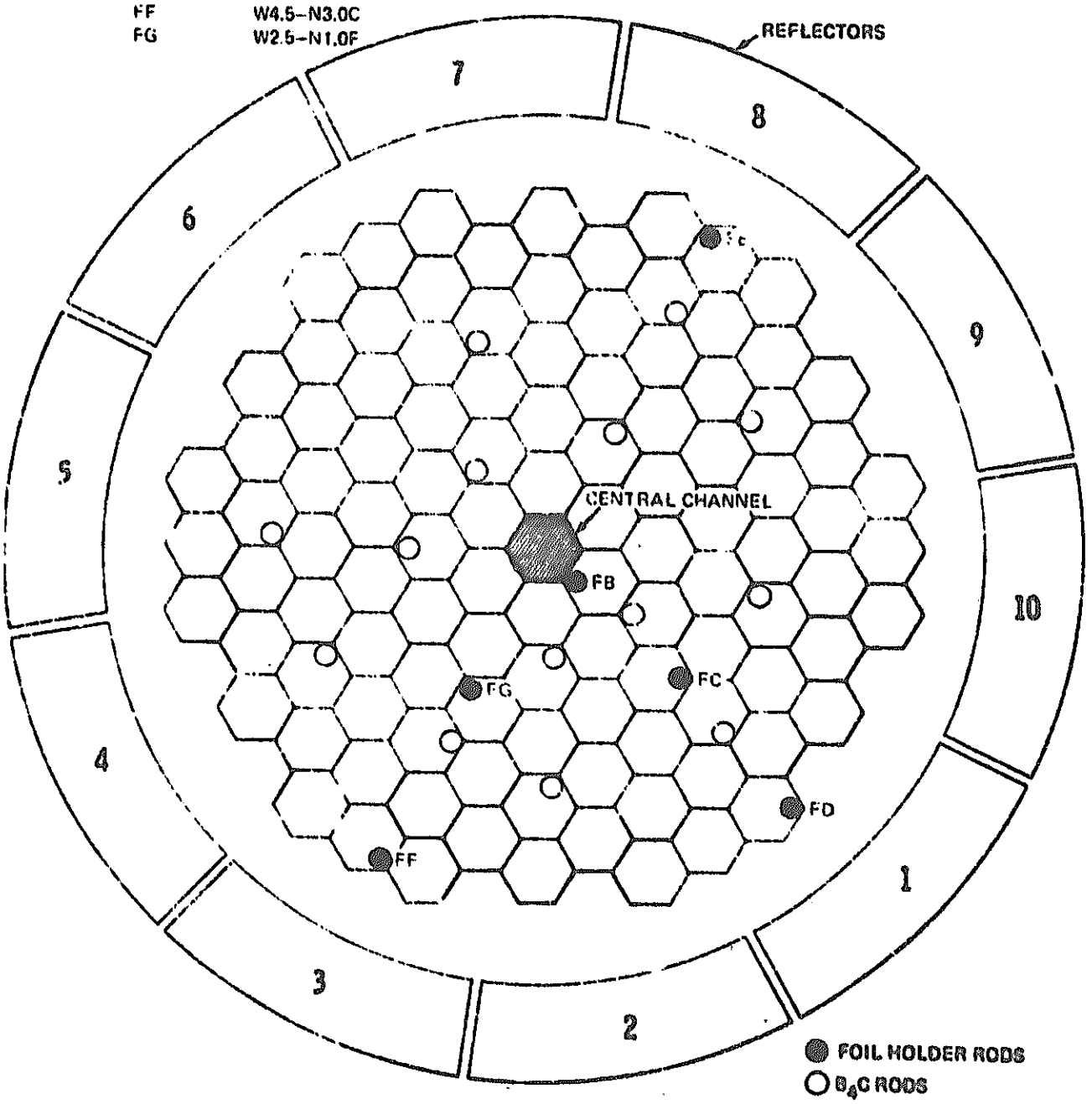

Figure 1. Foil Holder Rod Locations (Assembly 1-D)

TABLE 3

FISSION RATE MEASUREMENTS FOR Pu FOILS

(Relative Values)

Rod Number		FB	FG	FC	FF	FE	FD
Radial Distance*(cm)		5.8	19.6	23.2	43.3	43.3	44.5
Axial Position							
No.	Distance** (cm)						
8	90.8	0.6013	-	-	-	-	-
7	73.5	0.7388	-	-	-	-	-
6	58.2	0.9198	-	-	-	-	-
5	54.9	0.9396	-	-	0.5769	-	0.5871
4	53.0	0.9423	-	-	-	-	-
3	37.0	1.0000+	0.8564	0.8111	0.5543	-	0.5747
2	26.1	0.9419	-	-	-	-	-
1	1.2	0.6901	-	-	-	-	-

* Distance from core center

** Distance above bottom of core - core height = 91.2 cm

\+ The specific activity at this point was 6398.3 counts/min/mg.

TABLE 4

FISSION RATE MEASUREMENTS
FOR ENRICHED URANIUM FOILS

(Relative Values)

Rod Number		FB	FG	FC	FF	FE	FD
Radial Distance*(cm)		5.8	19.6	23.2	43.3	43.3	44.5
Axial Position							
No.	Distance** (cm)						
8	90.8	0.6240	0.5418	0.5018	-	-	-
7	73.5	0.7778	0.6629	0.6184	0.4311	-	0.4747
6	58.2	0.9515	0.8222	0.7807	0.5673	-	0.6055
5	54.9	0.9750	0.8679	0.8093	0.5979	0.5003	0.6114
4	53.0	0.9932	0.8806	0.7949	0.5953	-	0.6001
3	37.0	1.0000+	0.8599	0.8154	0.5703	0.5450	0.5782
2	26.1	0.9633	0.8524	0.7742	0.5275	-	0.5523
1	1.2	0.7191	0.6114	0.5739	-	-	-

* Distance from core center.

** Distance above bottom of core - core height = 91.2 cm.

\+ The specific activity at this point was 6410.2 counts/min/mg.

TABLE 5

FISSION RATE MEASUREMENTS
FOR DEPLETED URANIUM FOILS

(Relative Values)

Rod Number		FB	FG	FC	FF	FE	FD
Radial Distance*(cm)		5.8	19.6	23.2	43.3	43.3	44.5
Axial Position							
No.	Distance** (cm)						
8	90.8	0.4156	0.3667	0.3453	-	-	-
7	73.5	0.7032	0.6503	0.6075	0.3185	-	0.2875
6	58.2	0.7873	0.7179	0.6607	0.3607	-	0.3485
5	54.9	0.7825	0.6976	0.6365	0.3638	0.3177	0.3360
4	53.0	0.7743	0.6976	0.6729	0.3684	-	0.3555
3	37.0	1.0000+	0.8873	0.8345	0.4205	0.4151	-
2	26.1	0.9476	0.8713	0.8085	0.4051	-	0.3806
1	1.2	0.5165	0.4601	0.4200	-	-	-

* Distance from core center.

** Distance above bottom of core - core height = 91.2 cm.

+ The specific activity at this point was 230.8 counts/min/mg.

5.2 - SEFOR-1 (cont'd)

Theoretical Analysis:

The calculation was performed with a core model for Assembly I-D that has six radial core zones described below.

Calculated Core Zone	No. of fuel and B_4C Rods
1st	Central dry well described in Fig. 8 in 2-SEFOR-1
2nd	36 fuel rods
3rd	67 fuel and 5 B_4C rods
4th	108 fuel rods
5th	135 fuel and 9 B_4C rods
6th	288 fuel rods

The fuel and B_4C were assumed to be uniformly distributed within their respective zones.

Calculations using the above model were performed in 13 energy groups using two-dimensional synthesis, as well as true two-dimensional diffusion (2D) programs. There were no significant differences between the reaction rate distributions calculated with the two methods. Generally, however the reaction rate profiles obtained from the true 2D calculations were somewhat flatter than those calculated with the synthesis program. Infinitely dilute cross sections were used to calculate the fission rate distributions. The results of the true 2D calculations are shown in Figs. 3 through 10 with the experimental results.

In addition, the difference between the shape of the calculated axial U-238 fission distribution at a radius of 3.17 cm (in a calculational model this is in a sodium steel central channel region and is ∿1 cm from the inner radius of the fuel zone) and at 5.97 cm (or ∿1.7 cm within the fuel zone) is indicated by the fission rate ratios shown in Fig. 11. The calculations indicate that the difference in axial shape occurs within a distance of about 1 cm into the central channel and undergoes little additional change at further distance into the channel. Since the shortest distance between fuel rod centers is ∿2.8 cm, these calculations indicate that corrections should be applied to the calculations of the U-238 fission distribution to account for the absence of a fission source in the foil holder rods. Such corrections were applied by using the curve in Fig. 11 to obtain the calculated

curves in Figs. 4 and 7. Calculations indicated that no corrections of this nature were required for the U-235 and Pu-239 distributions.

The fission rates near the radial edge of the core are difficult to calculate because of the unusual geometry. With this model, for example, one of the foil holder rods (FD) is located at a radius (44.5cm) outside the periphery (44.1cm) of the core.

The measured values of the reaction rates in all the foils are higher, relative to the rates in the center, than the calculated values near the core reflector interfaces at the upper and lower boundaries of the core. Preliminary comparisons of two-dimmensional transport (S_4) and diffusion theory calculations indicate that corrections for transport effects would decrease these disparity by no more than $\sim$3%.

In general, the differences between the calculations and measurements are the order of 20% near the core boundaries, and the actual fission rate distribution may be slightly flatter than calculated.

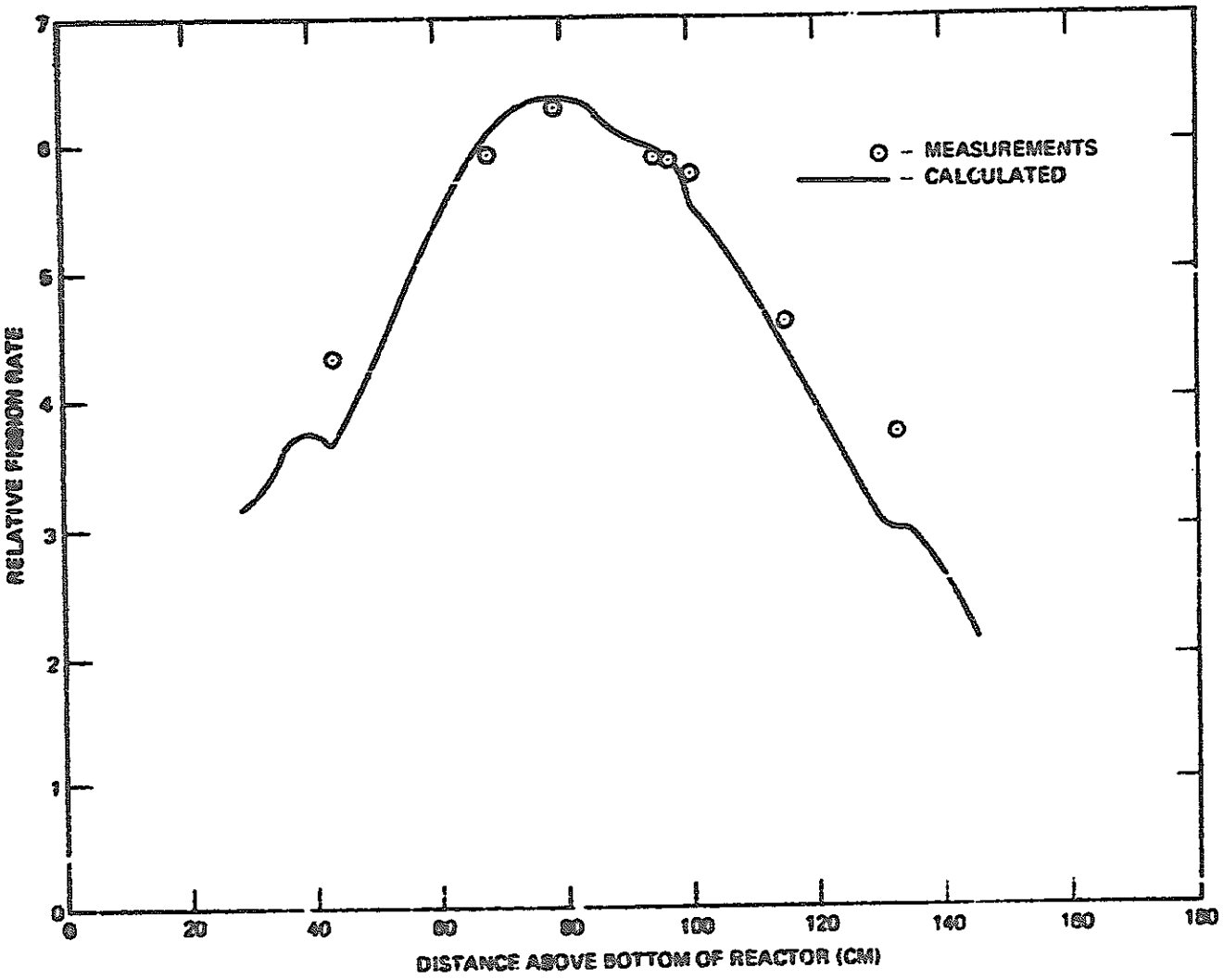

Figure 3. PU-239 Fission Distribution in Rod FB

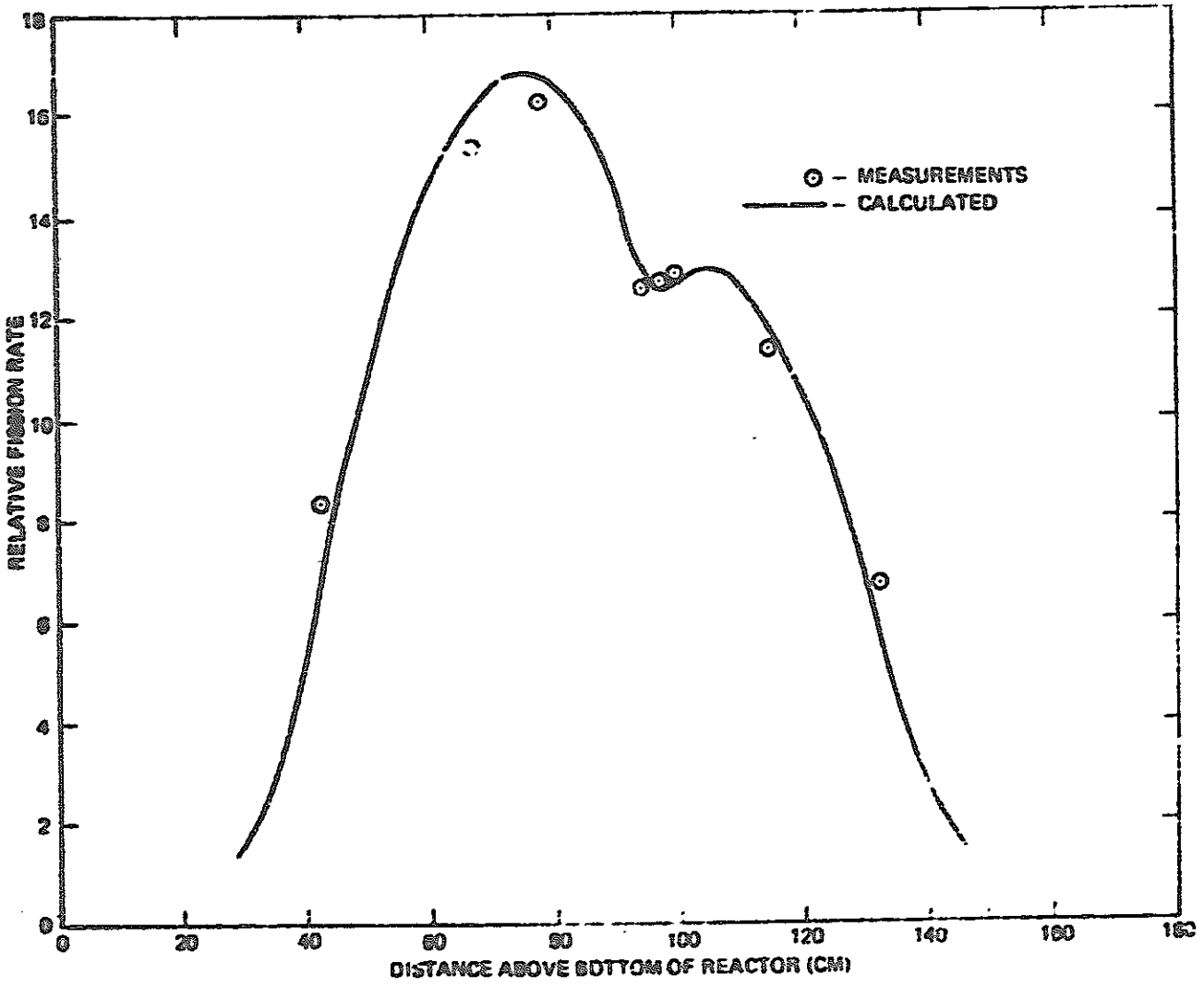

Figure 4. U-238 Fission Distribution in Rod FB

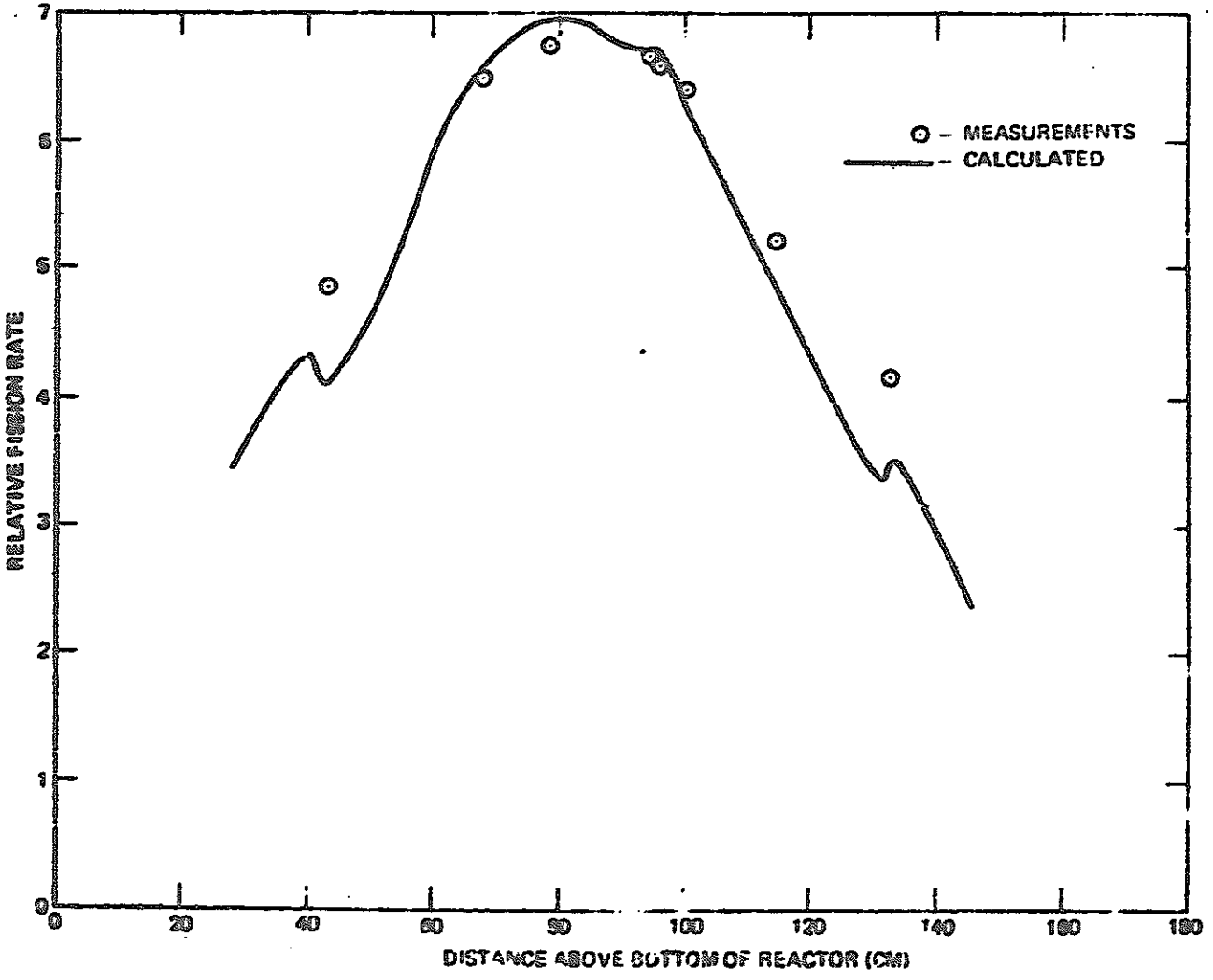

Figure 5. U-235 Fission Distribution in Rod FB

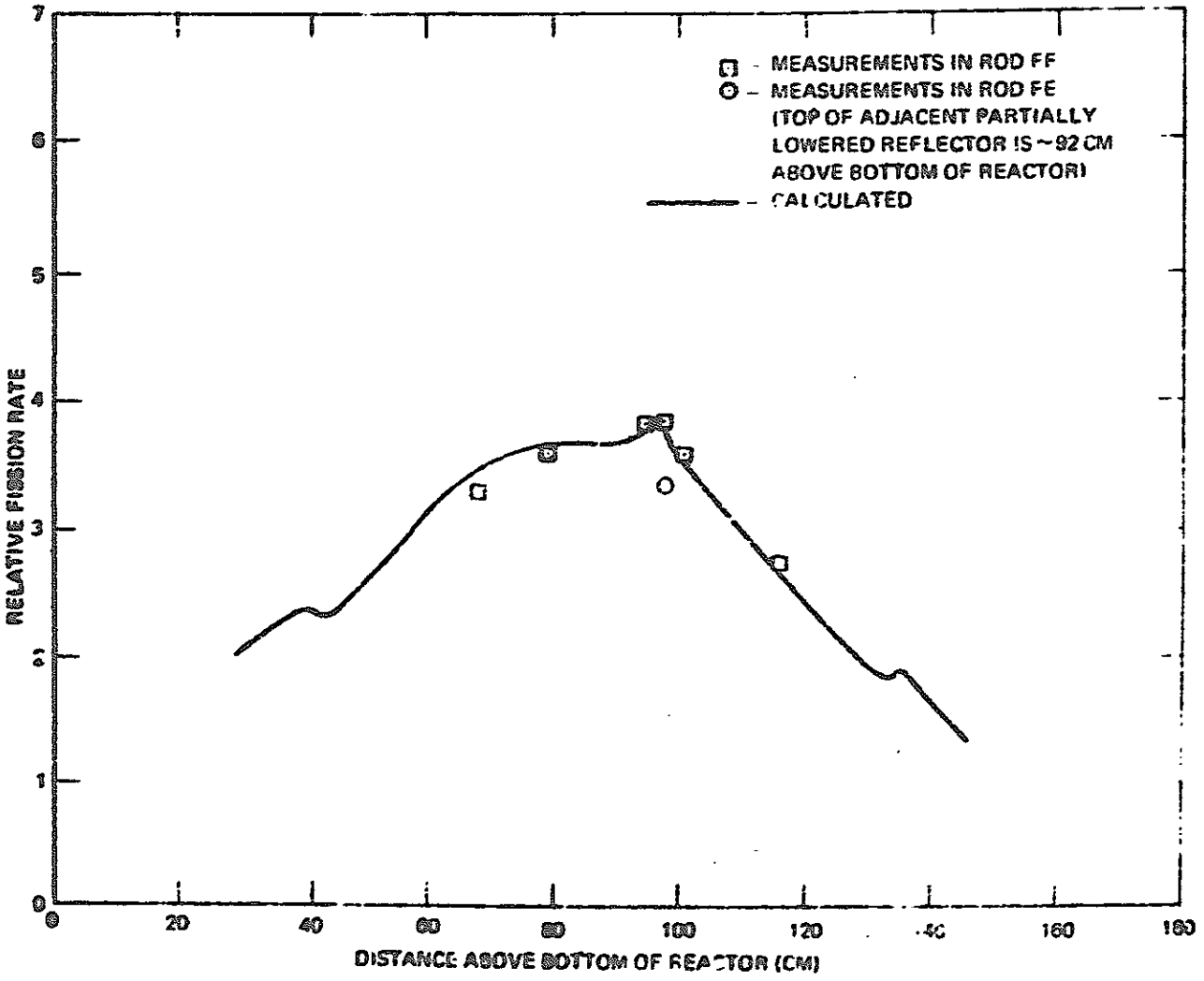

Figure 6. U-235 Axial Fission Distribution at Core Radial Boundary

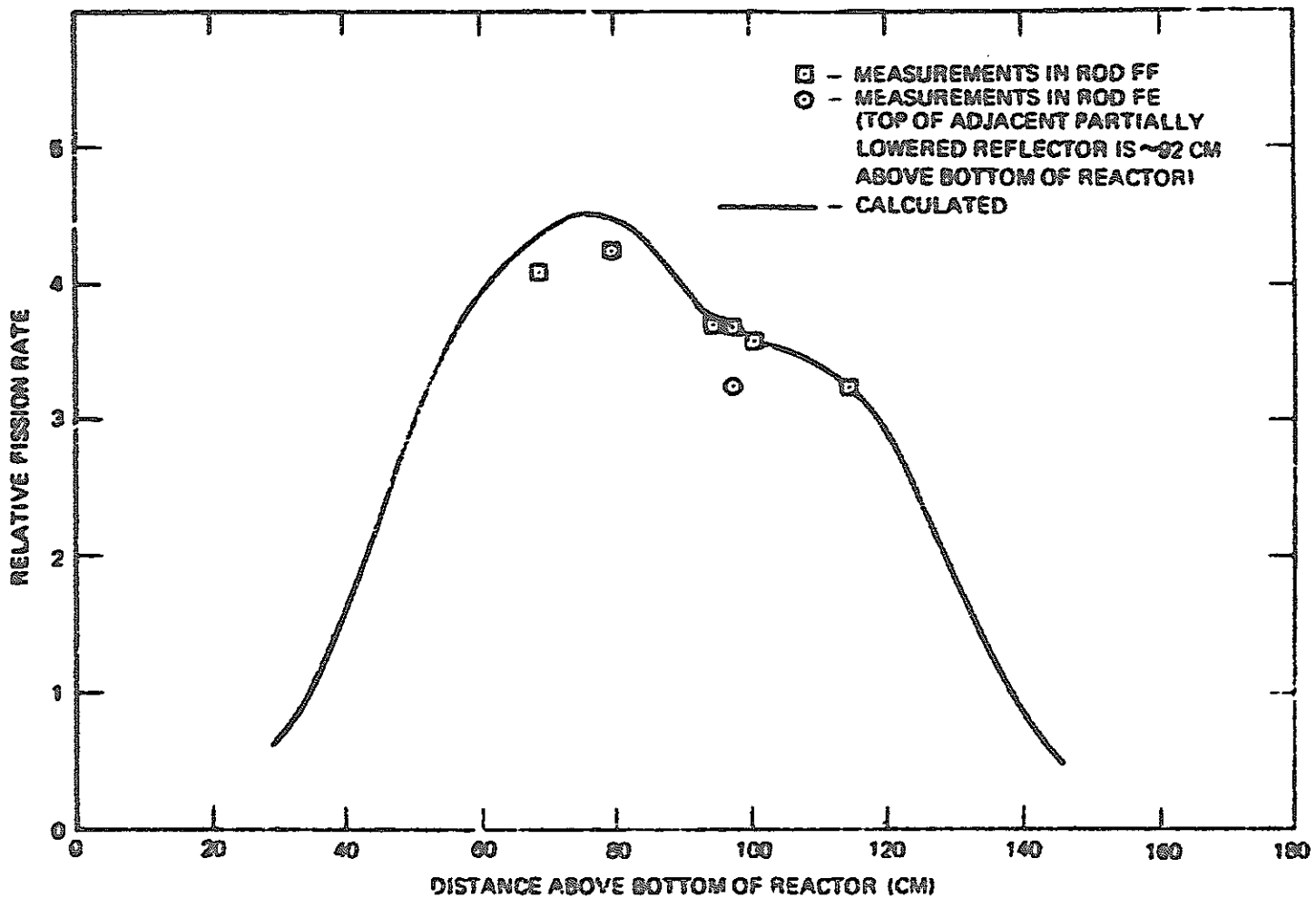

Figure 7. U-238 Axial Fission Distribution at Core Radial Boundary

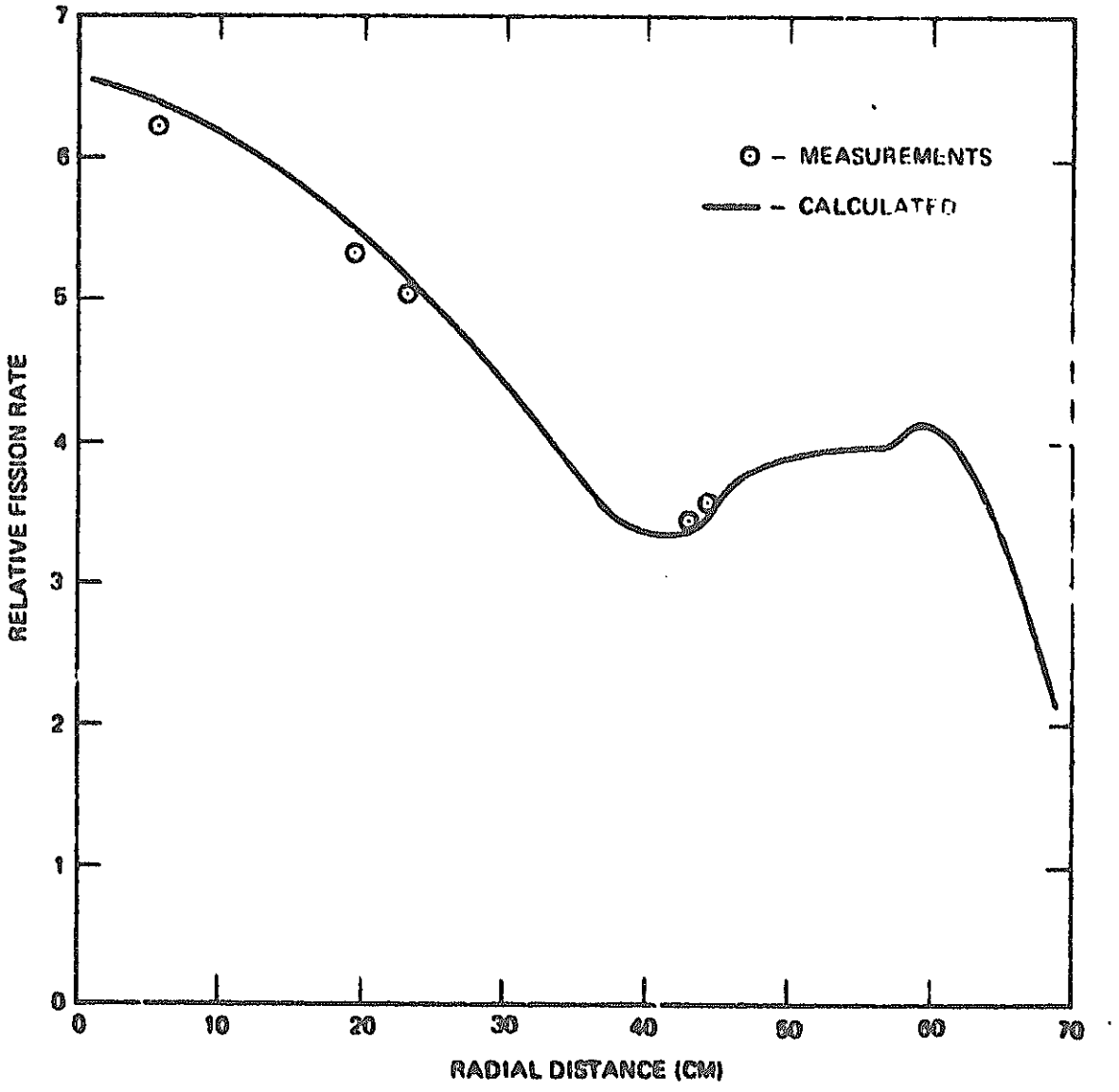

Figure 8. PU-239 Radial Fission Distribution at Axial Position 3

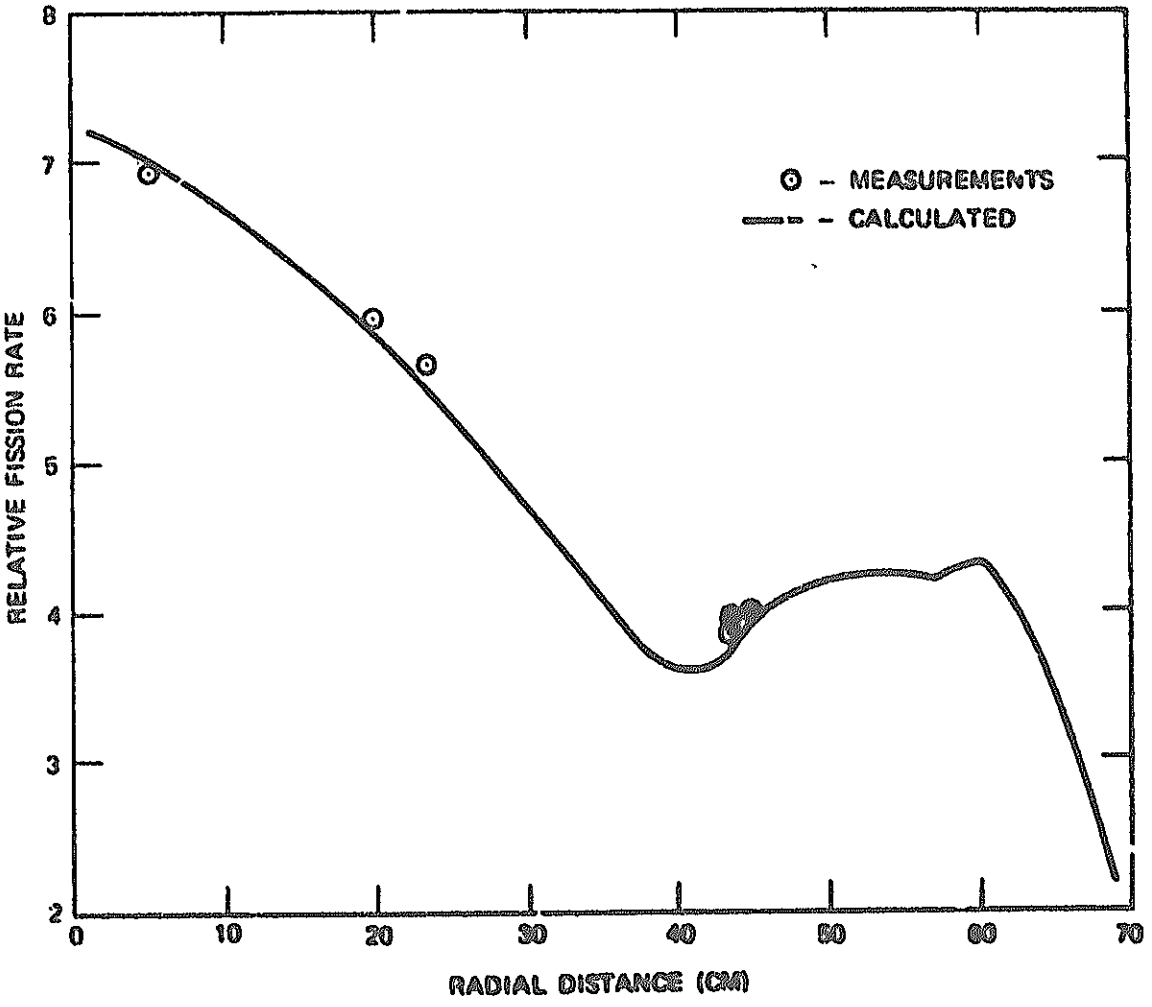

Figure 9. U-235 Radial Fission Distribution at Axial Position 3

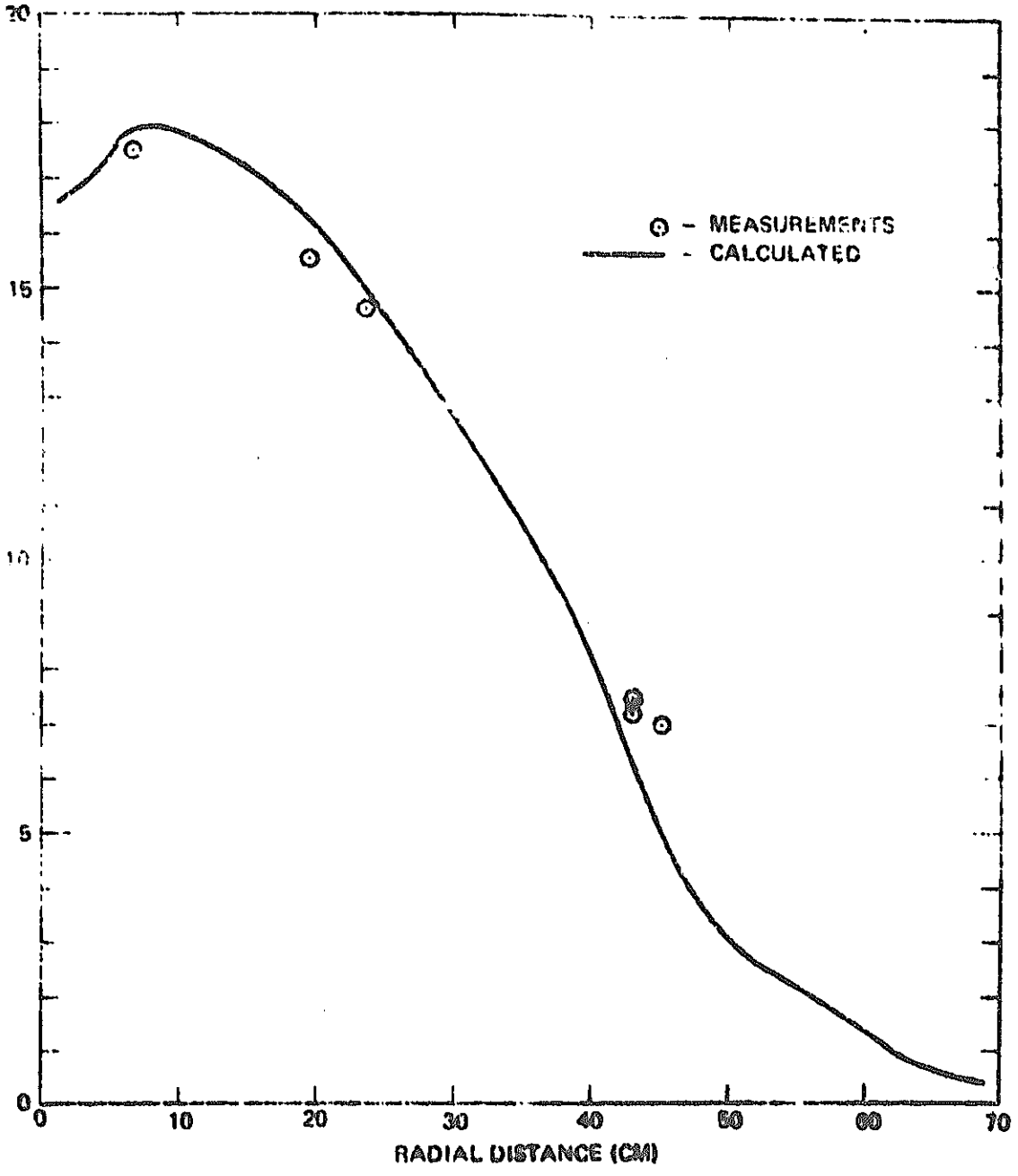

Figure 10. U-238 Radial Fission Distribution at Axial Position 3

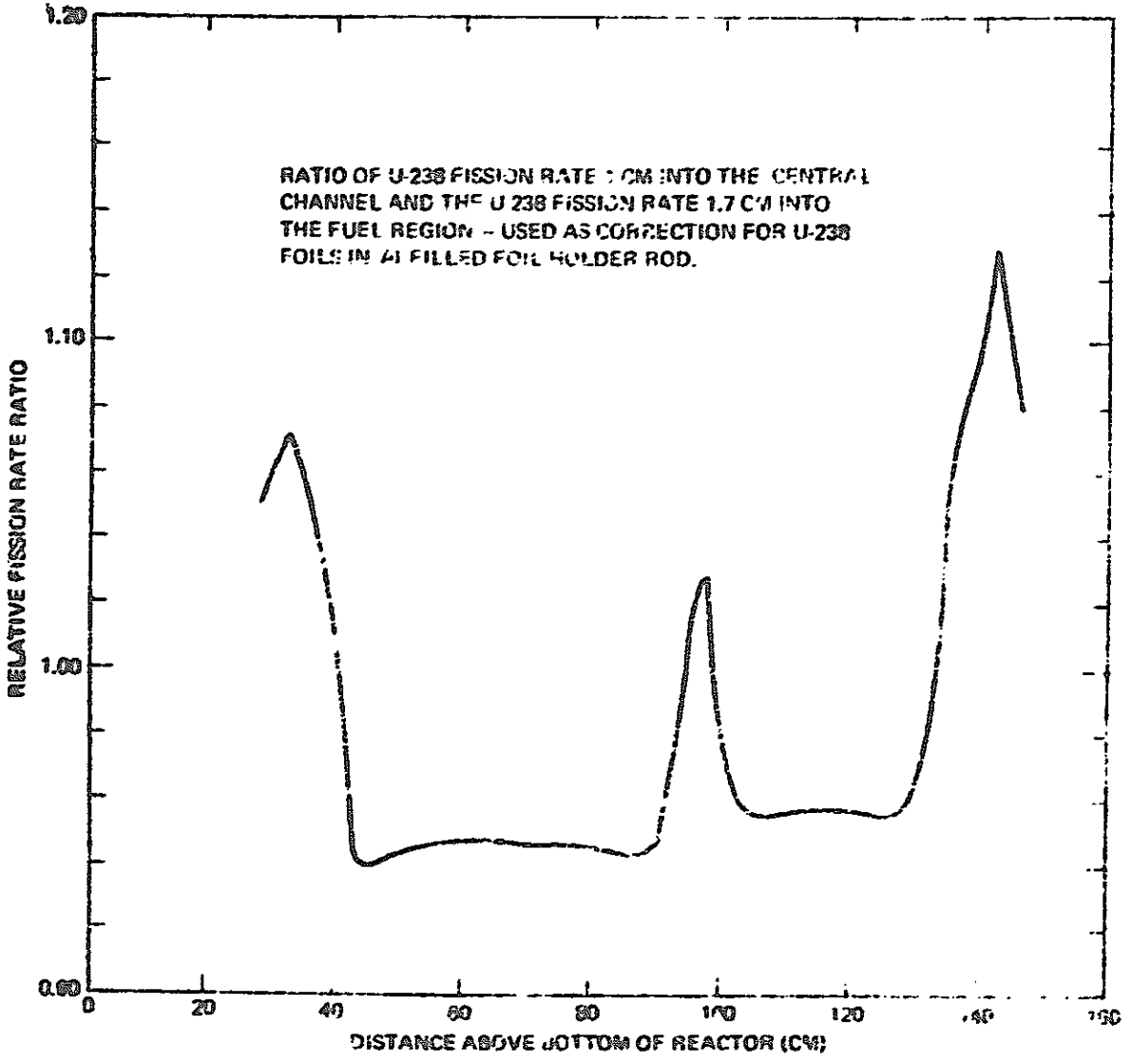

Figure 11. Ratio of U-238 Fission in the Central Channel and Adjacent Fuel Region

5.2 - SEFOR-1 (cont'd)

References:

1. L.D. Noble et al., GEAP-13588 (March, 1970) pp.87 - 112.

2. GEAP-5576 (Jan., 1968) pp.3.32 - 3.39.

3. GEAP-10010-23 (Nov., 1969 - Jan., 1970) pp.21 - 26.

4. GEAP-10010-24 (Feb. - April, 1970) pp.21 - 45.

7 - SEFOR-1 Doppler Coefficient

Facility: SEFOR Assembly: I

A. Experiment in Assembly I-I

Experimental Method:

The reactor power level was changed from zero to 5 MW at a constant coolant temperature of 760°F. Thermocouples (T/C's) were used to measure fuel temperature changes at seven different core locations. The thermocouples are located along the center line of four different fuel rods in two instrumented fuel assemblies (IFA's). All of the fuel thermocouples are located at one of two axial positions; either 2-1/4 inches or 15-1/2 inches above the midplane of the 36 inch high core. Those near the midplane will be refered to as lower T/C's, while those 15-1/2 inches above the midplane will be refered to as upper T/C's. One IFA was located near the core center line, and one near the periphery as shown in Figure 1. As indicated in Figure 1, each IFA contains an "inner fuel rod" and an "outer fuel rod", with the inner rod being that closest to the core center line.

Results:

The reflector positions, average core coolant temperature and power levels obtained during initial reactor operation up to 5 MW are listed in Table 1, along with measured power reactivity effects corrected for coolant temperature differences. The power levels and average coolant temperatures in Table 1 were calculated from the observed primary system flows and temperatures shown in Table 2.

The estimated Doppler effect is listed in Table 3. These values were obtained from Table 1 by correcting the calculated fuel axial expansion reactivity effect of -0.5 ¢/MW. The fuel temperature measurements from the seven T/C's are listed in Table 4.

TABLE 1

POWER REACTIVITY DATA

Reflector No. 3		Reflector No. 8		Average Core Coolant Temperature[2] (°F)	Temperature* Reactivity Correction (cents)	Power[3] (MW)	Reactivity** Effects due to Power Changes[1] (cents)
Position (cm)	Worth (cents)	Position (cm)	Worth (cents)				
0	0	-	52.62*	760.0*	0.0	0	0
0	0	37.61	51.58	744.0	-8.80	0.4	- 7.76
0	0	41.04	58.27	745.5	-7.98	0.8	-13.63
0	0	48.16	72.22	763.2	1.76	1.0	-17.84
17.0	16.70	40.00	56.22	763.2	1.76	1.0	-18.54
16.76	16.37	47.00	69.97	759.1	-0.50	2.0	-34.22
42.20	61.14	47.00	69.97	760.8	0.44	5.0	-78.05

* Reactivity temperature corrections were made with a coefficient of -0.55 cents/°F.

** This represents the change in core reactivity as the power is increased from zero and the average core coolant temperature is maintained at 760°F.

1 The estimated standard deviation in the reactivity effect is ±1.0 cents due to temperature deviations, with an additional -3% uncertainty due to reflector interaction effects.

2 The estimated standard deviation in temperature readings is ±1.5°F.

3 Preliminary estimate of the standard deviation in power is ±0.2MW or ±10%, whichever is larger.

TABLE 2

HEAT BALANCE DATA

Main Primary System			Auxiliary Primary System				
Flow[1] (gpm)	Inlet* Temperature[2] (°F)	Outlet Temperature[2] (°F)	Flow[1] (gpm)	Inlet* Temperature[2] (°F)	Outlet Temperature[2] (°F)	Power[3] (MW)	Average Core Temperature[2] (°F)
1987	741.2	746.2	185	747.2	748.4	0.4	744.0
1995	740.5	750.1	185	744.7	752.8	0.8	745.5
1998	757.2	769.0	185	758.7	771.7	1.0	763.2
2189	747.8	769.8	182	755.1	772.4	2.0	759.1
2326	734.1	787.1	180	743.3	786.3	5.0	760.8

* The recorded main primary inlet and auxiliary primary inlet temperatures have been decreased by 2°F and 1°F respectively to account for differences between inlet and outlet temperature readings at zero power.

1 These are average values. Flow variations were of the order of 1%.

2 The estimated standard deviation in temperature readings is ±1.5°F.

3 The standard deviation in power has yet to be determined. Preliminary estimaters are ±0.2MW or ±10%, whichever is larger.

TABLE 3

PRELIMINARY ESTIMATE OF MEASURED
DOPPLER REACTIVITY EFFECTS

Power (MW)	Estimated Doppler Effect* (cents)
0.0	0.0
0.4	- 7.6
0.8	-13.2
1.0	-17.3
1.0	-18.0
2.0	-33.2
5.0	-75.6

* These values include corrections for the calculated fuel and fuel clad axial expansion effect of -0.5 cents/MW, and corrections for changes in core average coolant temperature. Small additional corrections may be required to account for changes in reflector temperature and core inlet temperature. The measurement uncertainties and indicated in Table 1.

TABLE 4

IFA FUEL ROD TEMPERATURES

	Fuel Temperature Rise Above the Sodium Temperature**							
	Central IFA				Peripheral IFA			
	Inner Fuel Rod		Outer Fuel Rod		Inner Fuel Rod		Outer Fuel Rod	
Power (MW)	Upper T/C* (°F)	Lower T/C (°F)	Upper T/C (°F)	Lower T/C (°F)	Upper T/C (°F)	Lower T/C (°F)	Upper T/C+ (°F)	Lower T/C (°F)
0	0	0	0	0	0	0	-	0
0.4	52	82	-	85	35	68	-	56
0.8	75	135	-	137	61	104	-	90
1.0	108	166	105	176	77	133	-	116
2.0	197	-	192	329	140	246	-	208
5.0	471	822	477	864	-	636	-	529
Average Increase per Megawatt	94.4	165	95.8	172	75.0	127	-	106

* These are average values. This T/C was noisy with 20 to 30°F temperature fluctuations. The other T/C's demonstrated little or no fluctuations.

\+ This is a dummy thermocouple (T/C) that is used to account for any spurious signals.

** The average sodium temperature ranged between -740 and 760°F.

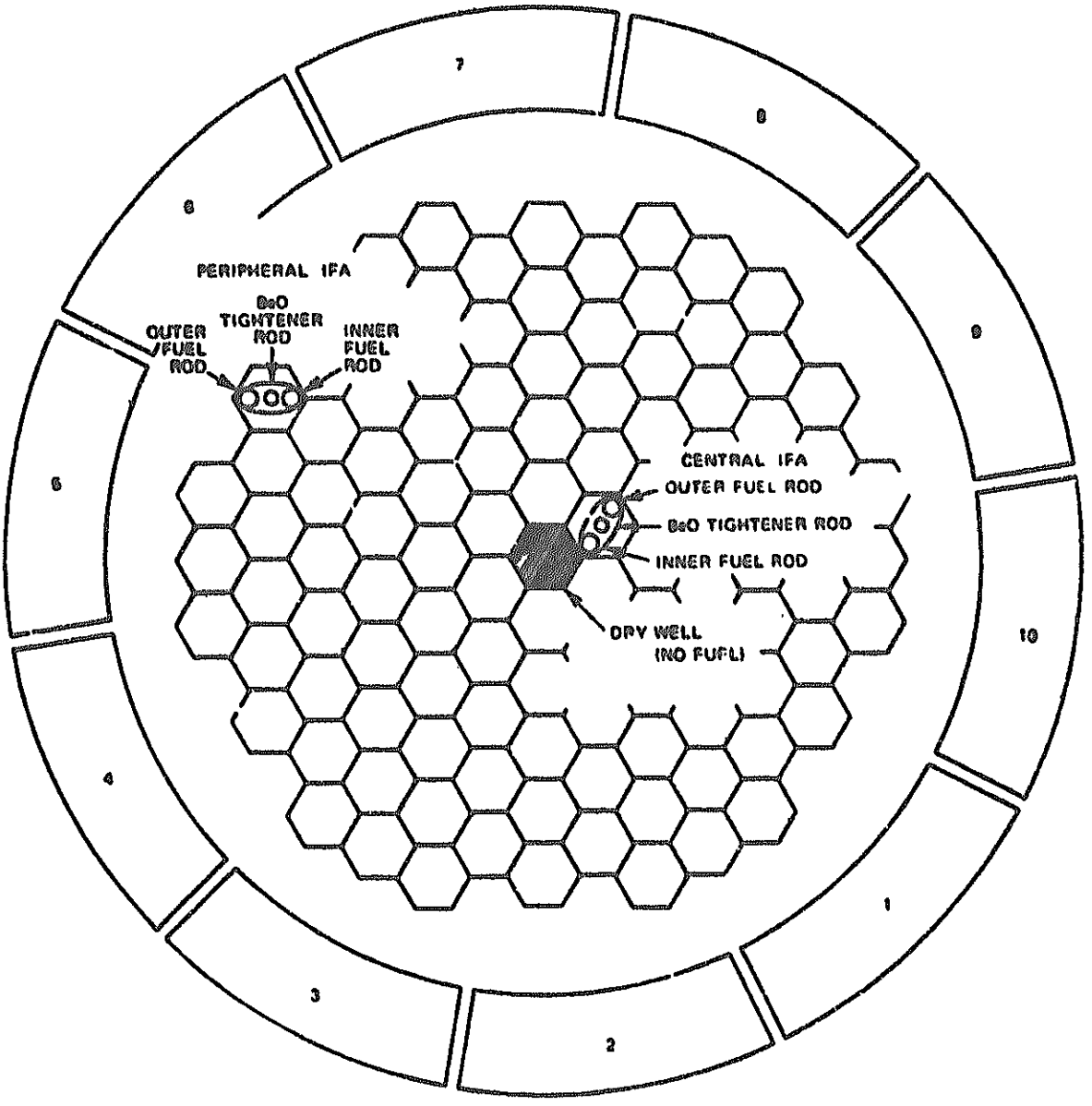

Figure 1. Instrumented Fuel Assembly (IFA) Locations in Assembly I-I

B. Experiments in Assembly I-J

Experimental Method:

Same as for Assembly I-I. An exception is that the reactor power level was changed from zero to 17 MW.

Results:

The measured increase in fuel temperature with power are tabulated in Table 5. All of the data in Table 5 was taken with an average core sodium temperature of ∿760°F, except for the few measurements which are noted in the Table. Above 10 MW T/C #2 became somewhat erratic as indicated by the data.

Table 6 shows the reactivity effects due to power changes at a constant average coolant temperature of 760°F. These tabulated reactivity values have been corrected for the variation in average sodium temperature using previously measured reactivity temperature coefficients and an approximation to the theoretical dependence of the average core coolant temperature reactivity coefficient on reactor power. Some of the values in Table 6 are averages of measurements performed over a time interval of several days. The thermal power levels and average coolant temperatures were calculated using the actual flow and temperature data (see Reference 3). Although all the static points in Table 6 were obtained at essentially the same average core coolant temperature and power level, the coolant inlet temperatures (flow) were not always the same. As the result of some experimental investigations any reactivity effect associated with the effect of change in sodium inlet temperature is less than the estimated standard deviation in reactivity (± 1.5¢ or 4% whichever is larger), and may be neglected.

The experimented Doppler components of the power reactivity effects are listed in Table 7. These values were obtained from Table 6 by correcting the calculated fuel and clad axial expansion reactivity effect of -0.5¢/MW.

TABLE 5

IFA FUEL ROD TEMPERATURES

Date (1970)	Thermal Power (MW)	Fuel Temperature Rise Above Sodium Coolant Temperature of ∿760°F — Central IFA — Inner Fuel Rod — Upper T/C #1 (°F)	Central IFA — Inner Fuel Rod — Lower T/C #2 (°F)	Central IFA — Outer Fuel Rod — Upper T/C #3 (°F)	Central IFA — Outer Fuel Rod — Lower T/C #4 (°F)	Peripheral — Inner Fuel Rod — Upper T/C #17 (°F)	Peripheral — Inner Fuel Rod — Lower T/C #18 (°F)	Peripheral — Outer Fuel Rod — Lower T/C #20 (°F)
7/2	0.4	52	82	-	85	35	68	56
7/2	0.8	75	135	-	137	61	104	90
7/2	1.0	108	166	105	176	77	133	116
7/3	2.0	197	-	192	329	140	246	208
7/9	5.0	471	822	477	864	-	636	529
7/9	5.1	475	816	487	870	-	641	541
7/10	5.2	507	824	487	862	-	640	540
7/10	5.1	507	824	487	860	-	646	544
7/10	5.2	495	822	477	875	-	643	534
7/11	5.0	466	760	446	808	-	608	506
7/23	5.0	472	804	-	830	-	702	574
7/24	5.2	448	737	-	753	-	662	540
7/27*	5.2	453	750	-	769	-	710	564
7/27*	5.4	467	780	-	799	-	734	585
7/27**	5.4	463	775	-	792	-	752	598
7/28+	5.8	503	842	-	861	-	835	658
8/6	2.2	199	294	-	317	-	344	282
8/7	5.2	470	790	-	803	-	808	664
8/14	4.9	454	770	-	773	-	831	678
8/14	6.0	554	962	-	964	-	991	832
8/14	7.0	640	1123	-	1044	-	1119	966
8/14	8.0	724	1289	-	1364	-	1254	1090
8/14	9.1	824	1490	-	1578	-	1360	1236
8/14	10.1	902	1671	-	1748	-	1506	1343
8/15	10.1	884	1435	-	1774	-	1669	1317
8/17	9.9	872	1390	-	1772	-	1704	1327
8/18++	10.0	841	1329	-	1772	-	1646	1279
8/23	5.1	436	651	-	-	-	967	754
8/29	10.1	898	1365	-	1756	-	1753	1427

* Average core sodium temperature is ∿600°F.

** Average core sodium temperature is ∿500°F.

\+ Average core sodium temperature is ∿400°F.

++ Average core sodium temperature is ∿560°F.

TABLE 5 (continued)

FUEL TEMPERATURE RISE ABOVE SODIUM COOLANT TEMPERATURE OF ~760°F

Date (1970)	Thermal Power (MW)	Central IFA			Peripheral IFA	
		Inner Fuel Rod		Outer Fuel Rod	Inner Fuel Rod	Outer Fuel Rod
		Upper T/C#1 (°F)	Lower T/C#2 (°F)	Lower T/C#4 (°F)	Lower T/C#18 (°F)	Lower T/G#20 (°F)
8/29	11.2	973	1525	1834	1728	1520
8/29	12.5	1076	2021	2306	1691	1643
8/29	13.2	1145	2144	2487	1554	1736
8/29	14.0	1213	2292	2834	1499	1825
8/29	15.5	1383	2559	2761	1820	1967
8/29	14.8	1329	2351	2703	2095	1903
8/30	14.8	1343	1337	1957	2099	1920
8/30	15.1	1352	1331	1239	2262	1948
9/4	9.9	852	847	1491	1690	1426
9/5	10.0	828	840	1564	1720	1425
9/5	15.0	1305	1325	1934	2214	1969
9/5	15.0	1290	1315	1818	2170	1960
9/5	17.2	1612	1340	1805	1898	2177
9/6	17.2	1561	1307	1270	2251	2182

TABLE 6

POWER REACTIVITY DATA

Date (1970)	Reflector #3 Position (cm)	Reflector #3 Worth (¢)	Reflector #8 Position (cm)	Reflector #8 Worth (¢)	Average Core Coolant Temperature (°F)	Thermal Power (MW)	Neutron Instrumentation (MW)	Reactivity Change* at 760°F Average Coolant Temperature (¢)
6/30-7/8	0	0	-	52.62+	760.0+	0	-	0
7/2	0	0	37.61	51.58	744.0	0.4	0.5	- 7.8
7/2	0	0	41.04	58.27	745.5	0.8	0.9	- 13.6
7/2	0	0	48.16	72.22	763.2	1.0	1.1	- 17.9
7/2	17.0	16.70	40.00	56.22	763.2	1.0	1.1	- 18.6
7/3	16.76	16.37	47.00	69.97	759.1	2.0	2.0	- 34.2
7/9-7/24	-	60.82+	47.00+	69.97+	760.0+	5.1+	5.1+	- 78.2+
8/6-8/16	-	-	-	58.06+	760.0+	0	-	0
8/6	18.79	19.24	47.00	89.97	759.6	2.2	2.0	- 31.4
8/7	43.70	64.02	47.00	69.97	760.1	5.2	5.1	- 75.9
8/14	42.32	61.37	47.01	69.99	758.1	4.9	5.0	- 74.3
8/14	50.83	77.70	47.01	69.99	763.7	6.0	6.1	- 87.8
8/14	57.43	89.60	47.01	69.99	765.2	7.0	7.2	- 98.9
8/14	62.11	97.72	47.01	69.99	760.6	8.0	8.1	-109.3
8/14	70.00	110.23	47.07	70.11	760.2	9.1	9.3	-122.2
8/14-8/17	70.00+	110.23+	-	78.92+	760.0+	10.0+	10.2+	-131.1+
8/23-8/30	0	0	-	21.96+	760.0+	0	-	0
8/23	40.00	56.91	30.82	38.84	759.7	5.1	5.2	- 74.0
8/29	40.00	56.91	58.63	91.70	758.3	10.1	10.2	-127.5
8/29	40.00	56.91	64.00	100.78	759.6	11.2	11.1	-135.9
8/29	40.20	57.30	70.00	110.02	758.0	12.5	12.4	-146.3
8/29	43.35	63.35	70.00	110.02	757.4	13.2	13.2	-152.3
8/29	46.89	70.17	70.00	110.02	757.5	14.0	14.0	-159.4
8/29	53.48	82.59	70.00	110.02	759.4	15.5	15.3	-170.9
8/29	51.42	78.90	70.00	110.02	759.5	14.8	14.8	-167.2
8/30	50.19	76.50	70.00	110.02	756.2	14.8	14.9	-166.4
8/30	51.19	78.38	70.00	110.02	758.9	15.1	15.2	-170.0
9/4	57.50	89.72	40.00	56.22	762.2	9.9	10.0	-122.9
9/5	56.39	91.29	40.00	56.22	760.4	10.1	10.1	-125.4
9/5	50.57	77.21	70.00	110.02	756.1	15.0	15.1	-167.5
9/5	50.81	77.66	70.00	110.02	756.2	15.0	15.1	-184.3
9/5	61.00	95.85	70.00	110.02	759.1	17.2	17.4	-184.3
9/6	60.70	95.34	70.00	110.02	757.7	17.2	17.3	-184.5

* Reactivity-temperature corrections made using a reactivity coefficient of $\left[\frac{-0.36 - 0.10(1220)}{1220 + 65P}\right]$¢/°F at power level P(MW).

\+ See reference 3.

TABLE 7

DOPPLER COMPONENT OF MEASURED
POWER-REACTIVITY EFFECTS

Date (1970)	Thermal Power (MW)	Doppler Effect* (¢)
7/2	0.0	0.0
7/2	0.4	- 7.6
7/2	0.8	- 13.2
7/2	1.0	- 17.4
7/2	1.0	- 18.1
7/3	2.0	- 33.2
7/9-7/24	5.1	- 75.6
8/6-8/16	0.0	0.0
8/6	2.2	- 30.2
8/7	5.2	- 73.3
8/14	4.9	- 71.9
8/14	6.0	- 84.5
8/14	7.0	- 95.0
8/14	8.0	-105.3
8/14	9.1	-117.1
8/14-8/17	10.0	-126.1
8/23-8/30	0.0	0.0
8/23	5.1	- 71.5
8/29	10.1	-122.5
8/29	11.2	-130.3
8/29	12.5	-140.1
8/29	13.2	-146.1
8/29	14.0	-152.4
8/29	15.5	-163.2
8/29	14.8	-159.8
8/30	14.8	-158.9
8/30	15.1	-159.4
9/4	9.9	-118.0
9/5	10.1	-120.3
9/5	15.0	-159.6
9/5	15.0	-160.0
9/5	17.2	-175.7
9/5	17.2	-175.9

* Obtained from the last column of Table 6 by accounting for the calculated fuel-fuel clad axial expansion reactivity effect of -0.5¢/MW. A preliminary estimate of the standard deviation in the Doppler reactivity values is ±2.0¢ or 5% whichever is larger. The preliminary estimate of the standard deviation in power is ±0.3 MW or 5% whichever is larger, for power level > 2 MW.

Theoretical Analysis:

1. Reactivity Coefficient at Zero Power

Calculations were performed for two fully loaded cores, one containing 629 fuel rods and 19 B_4C rods distributed uniformly through the core and the other containing 636 fuel rods and 12 B_4C rods. In addition, calculations were performed for a partially loaded core containing 512 fuel rods and no B_4C rods.

The results for U-238 Doppler effect are summarized in Table 8. The Doppler reactivity effects for the fully loaded cores were calculated by 13 energy group two-dimensional synthesis code BISYN and those for the partially loaded core by perturbation of a 60 energy group, one-dimensional radial diffusion theory calculation besides the above BISYN calculations.

The calculations indicate that for the fully loaded core the quantity defined as Tdk/dT can be treated as a constant (within $\sim$ ± 5%) over the temperature range between 300°K and 1400°K.

The predicted Doppler Tdk/dT is -0.0082 for a fully loaded core containing 19 uniformly distributed B_4C rods and -0.0086 for a partially loaded core containing 512 fuel rods and no B_4C rods. The predicted Tdk/dT for a fully loaded core containing 12 B_4C rods (including a contribution from Pu-240 of -0.0003) is -0.0086.

It was assumed that the Pu-239 contribution to the Doppler effect is zero.

For the discussion of the comparison with experimental results in Assembly I-E, see Theoretical Analysis in 8-SEFOR-1.

2. Reactivity Coefficient at Higher Power Level in Assembly I-J

The local reactivity effect introduced by local fuel temperature changes(+) was calculated by the WEDOP program under the assumptions that the local change in reactivity is proportional to the logarithm of the local temperature change. The total core Doppler reactivity changes were calculated using a power-squared weighting of the local reactivity effects.

The reactivity changes for a Doppler Tdk/dT of -0.0080 that were obtained from the WEDOP calculations are compared with the measured Doppler reactivity effects in Fig. 2. It is seen that the agreement between measured and calculated effects as a function of reactor power is quite good.

(+) The descriptions of the fuel thermal conductivity, fuel-to-clad gap coefficient, power distribution, etc. that relate total power to local fuel temperature are shown in Reference 3.

The WEDOP program was also used to calculate the Doppler component of the change in reactivity that occurs when the coolant temperature is changed while the power level is held constant. These calculated results were combined with the calculated non-Doppler coolant coefficient of -0.36 cents/°F (8-SEFOR-1) and are compared with the measured results in Table 9. As with the power reactivity measurements noted above, the agreement between calculations using a Doppler Tdk/dT of -0.0080 and experiment is good. In these cases, however, the Doppler effect is less than half the total measured change, and the comparison of the results is more dependent upon the magnitude of the non-Doppler contribution.

TABLE 8

U-238 DOPPLER CALCULATIONS

Number of B_4C rods in Fully Loaded Core	Reactivity Effects for Fully Loaded Core (using 13 energy groups and synthesis calculation) 300°K to 700°K Δk	700°K to 1400°K Δk	Average Tdk/dT (300°K to 1400°K)
19	-0.00695	-0.00518	-0.0079
12	-0.00726	-0.00541	-0.0083

Method of Calculation	Reactivity Effects for 512 Rod Partially Loaded Core 300°K to 700°K Δk	Doppler $T\frac{dk}{dT}$ (300°K to 700°K)
Perturbation of a 60-group radial problem	-0.00707	-0.00835
Change in reactivity from synthesis calculations	-0.00692	-0.00817
		Average = -0.0083

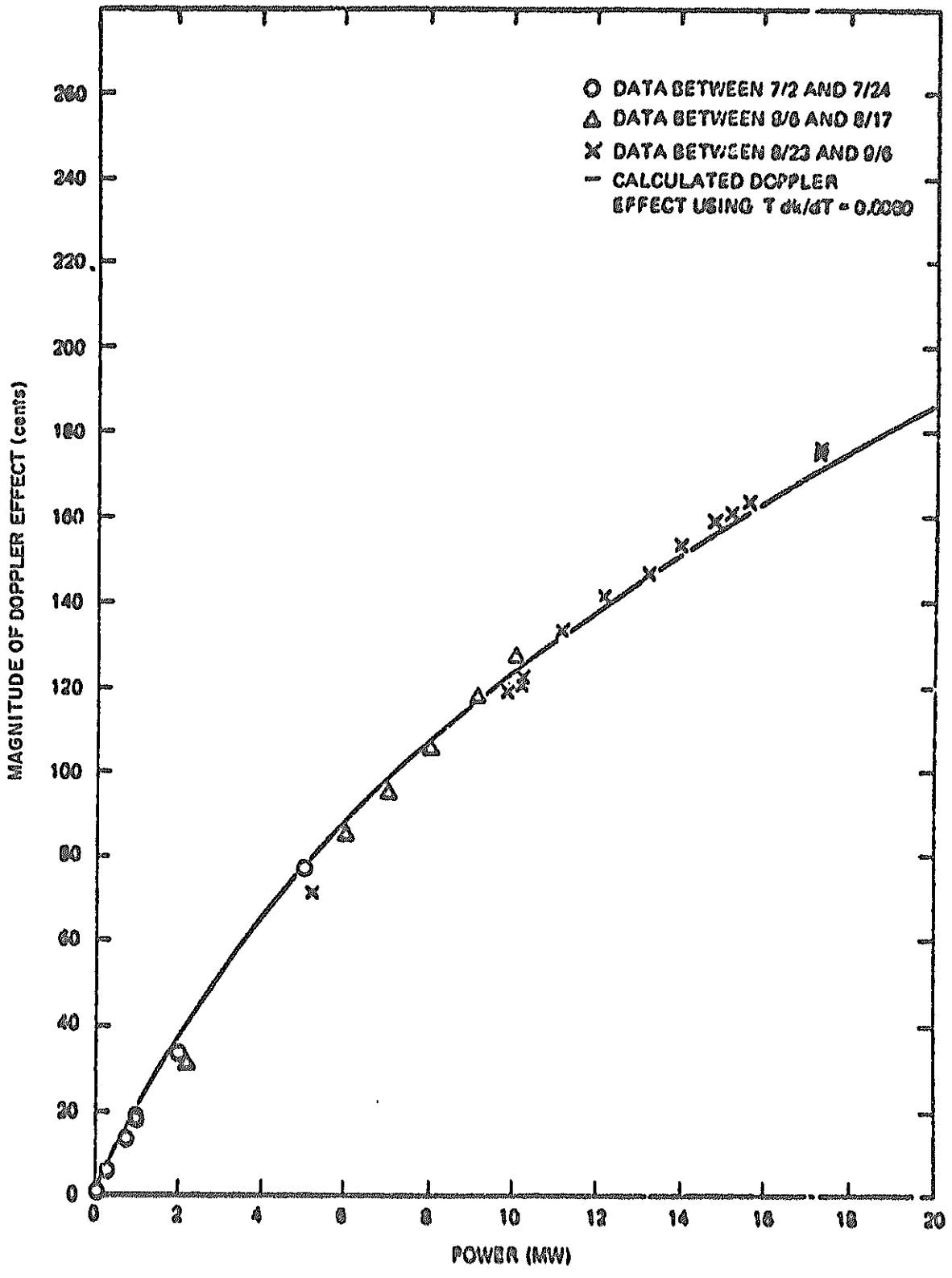

Figure 2. Doppler Power Reactivity Measurements

TABLE 9

MEASURED AND CALCULATED REACTIVITY EFFECTS AT CONSTANT POWER

Power (MW)	Average Core Coolant Temperature (°F)	Calculated[a] Non-Doppler Effect (cent)	Calculated[a] Doppler Effect (cent)	Total Reactivity Change	
				Calculated (cent)	Measured (cent)
0	760	0.0	0.0	0	0
0	650	39.6	24.0	64	63
0	550	75.6	48.0	124	123
0	350	147.6	104.0	252	254
5	760.0	0.0	0.0	0.0	0.0
5	604.0	56.2	27.3	83.5	85.3
5	603.6	56.3	27.6	83.9	85.6
5	500.6	93.4	47.6	141	142
5	401.8	129.0	69.1	198	202
10	760.0	0.0	0.0	0.0	0.0
10	559.4	72.2	33.8	106	106

a) The calculated total non-Doppler effect is a constant -0.36 cent/°F. The Doppler contribution was calculated with the WEDOP[4] program using a Doppler $T\frac{dk}{dT}$ of -0.0080.

Reference

1. GEAP-10010-21 (May-July, 1969) pp.45-49
2. GEAP-10010-25 (May-July, 1970) pp.6-14
3. GEAP-10010-26 (August-October, 1970) pp.15-37
4. L.D. Noble et al., GEAP-13588 (March, 1970) pp.137-160
5. R.A. Meyer et al., GEAP-13598 (June, 1970) pp.3.42-3.77
6. L.D.O'Dell, HEDL-TME 71-81 (May, 1971)

8 - SEFOR-1 Temperature Coefficients

Facility: SEFOR Assembly: I

A. Experiments in Assembly I-D

Experimental Method:

The reactor was operated at zero power and the primary sodium was heated from 350°F to 400°F by the primary trace heating system. The temperature was maintained at 400°F for about two hours and the primary system was then cooled down to 350°F. This process was repeated to establish the reproducibility of the data. The reactor was shut down during the actual heating and cooling periods, but steady state critical reflector positions were recorded at both temperature extremes.

Results:

The data obtained during the experiment are shown in Table 1. A least squares fit of a straight line to the data in the Table gives a value of -0.59 ± 0.01¢/°F for the temperature coefficient.

TABLE 1

TEMPERATURE COEFFICIENT MEASUREMENTS IN ASSEMBLY I-D

Temperature (°F)	Reflector #3 Position (cm)	Reflector #3 Worth* (¢)	Reflector #8 Position (cm)	Reflector #8 Worth* (¢)	Reactivity Change Relative to 350°F (¢)
352.0	0.75	0.19	52.09	74.02	-0.88
398.5	0.75	0.19	69.07	101.60	-28.46
397.5	0.75	0.19	68.88	101.33	-28.19
397.0	0.75	0.19	68.67	101.03	-27.89
350.0	0.44	0.00	51.71	73.33	0.00
398.25	0.44	0.00	69.27	101.88	-28.55
398.25	0.44	0.00	69.27	101.88	-28.55
398.25	0.44	0.00	69.15	101.71	-28.38
398.25	0.44	0.00	69.15	101.71	-28.38

* Relative to the worth with the reflector lowered.

B. Experiments in Assembly I-E

Experimental Method:

The reactor power level was held constant at about 600 watts throughout the heating and cooling by adjusting the reflector position to compensate the reactivity feedback effects.

The primary sodium temperature was stabilized for 2 - 3 hours at temperatures of approximately 450°F, 550°F, 650°F and 760°F to insure that both thermal and nuclear equilibrium were attained at these points. The temperature at each step was measured by the thermocouple located inside the reactor vessel and the Resistance-Temperature Detector (RTD's) located at the auxiliary and/or primary reactor inlet.

Results:

The reactivity feedback as a function of temperature is shown in Table 2 and Figure 1. The average temperature coefficients are shown in Table 3.

It will be seen in Figure of Reference 1 that there was no significant difference between inlet and outlet temperatures.

Precision:

The uncertainties in the measured reactivity changes were discussed in 4.2-SEFOR, and other source of uncertainty is considered to be ±4% due to "shadowing" (see Reference 1). The RTD readings had an estimated uncertainty at any point of ±2.5°F, while those in the thermocouple reading at any point was ±0.25°F.

TABLE 2

TEMPERATURE-REACTIVITY MEASUREMENTS

Temperature (°F)	Reactivity Change* (cents)	Temperature (°F)	Reactivity Change* (cents)
356.5	4.5	562.75	139.4
370.0	13.1	577.0	147.7
384.25	23.4	588.0	154.0
398.5	32.6	606.25	165.0
409.25	39.8	618.75	172.2
415.5	43.9	631.5	181.1
428.75	51.2	639.75	185.4
437.5	59.0	650.0	192.0
451.75	68.4	659.6	198.9
461.0	74.2	663.5	201.4
469.25	79.2	669.0	204.4
483.0	87.5	677.5	207.9
492.5	94.9	690.0	215.2
507.0	105.5	700.0	221.4
511.5	105.5	712.25	227.2
519.75	114.3	724.5	234.1
524.5	114.9	736.75	241.0
536.0	123.0	750.0	247.5
550.0	132.0	759.0	253.2

* Relative to a temperature of 350°F

TABLE 3

UNIFORM TEMPERATURE COEFFICIENT OF REACTIVITY
BETWEEN 350°F and 760°F

Temperature Range (°F)	Average Temperature Reactivity Coefficient in indicated Temperature Range (¢/°F)	
	Measured**	Predicted*
350 to 450	-0.67	-0.66
450 to 550	-0.64	-0.63
550 to 650	-0.60	-0.61
650 to 760	-0.57	-0.58

* The expression[3] for the coefficient at a given temperature T (in degrees Rankin) is $-(0.36 + 260/T)$ ¢/°F. (see discussion in Theoretical Analysis for the influence of B_4C content on the calculated coefficients).

** A fit to the experimental data yields a coefficient at a given temperature T (in degrees Fahrenheit) of the form - $[0.692 - 0.000357(T-350)]$ ¢/°F.

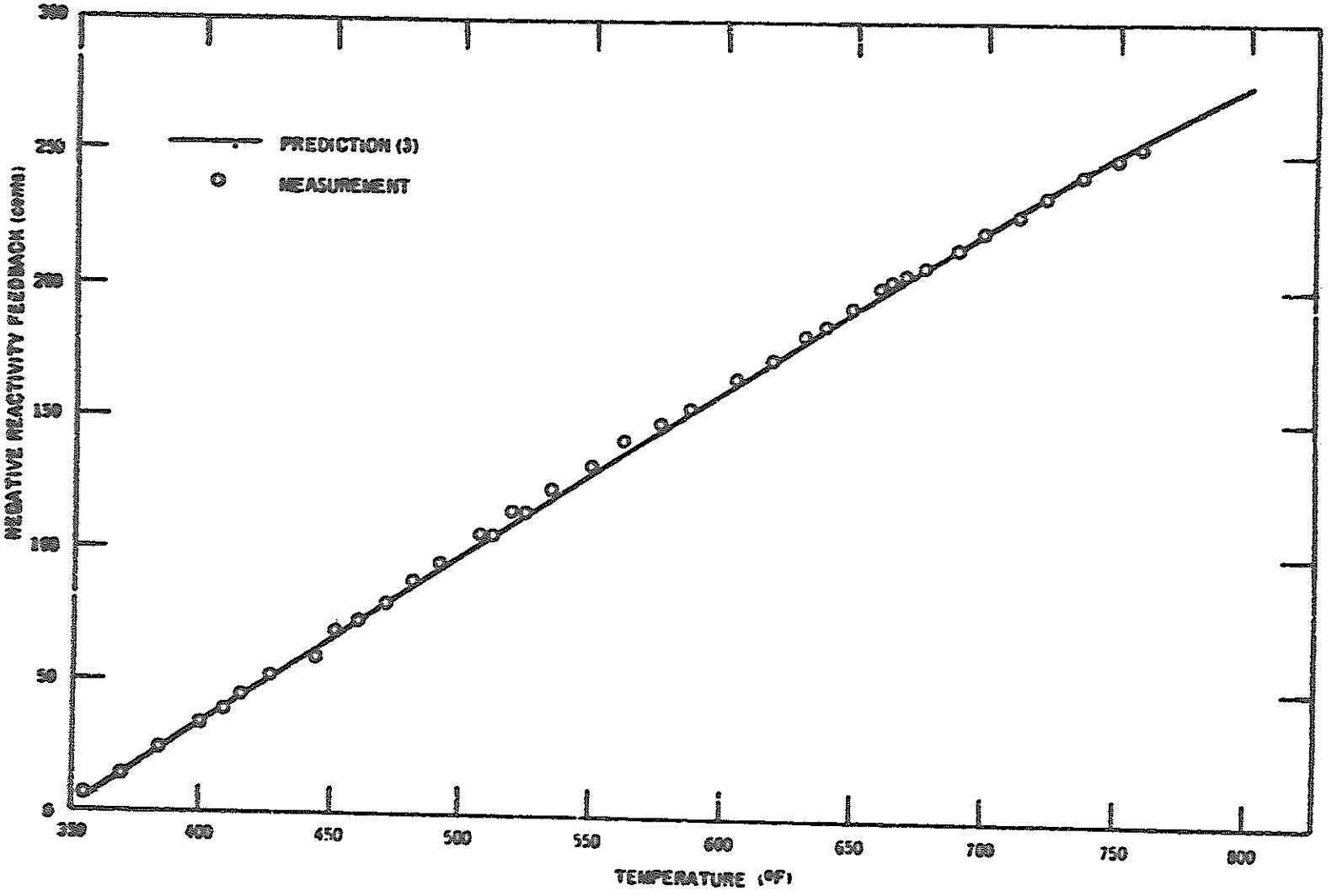

Figure 1. Temperature Reactivity Feedback (Assembly I-E)

8 - SEFOR-1 (cont'd)

C. Experiment in Assembly I-I

Experimental Method:

The temperature-dependent reactivity feedback between 360°F and 760°F at zero power was measured.

Results:

See Table 4.

TABLE 4

TEMPERATURE-REACTIVITY EFFECTS (360-760°F)

(Assembly I-I)

Reading Number	Reflector Position (cm)		Reactor Inlet+ Temperature (°F)	Negative Reactivity* Feedback (cents)
	No. 3	No. 8		
1	31	1.03	360	0.0
2	31	11.07	371	8.4
3	31	25.31	400	26.1
4	31	35.59	427	42.7
5	31	44.35	450	58.5
6	31	52.71	472	73.0
7	31	60.86	495	86.5
8	31	69.63	515	99.4
9	31	79.56	532	111.2
10	up	37.43	537	114.3
11	up	41.37	549	121.7
12	up	44.33	557	127.3
13	up	46.37	564	131.3
14	up	47.06	564	132.6
15	up	50.00	574	138.2
16	up	53.62	588	145.0
17	up	60.27	602	156.7
18	up	64.38	614	163.4
19	up	67.67	623	168.5
20	up	70.12	628	172.0
21	up	74.53	639	177.9

Reflector No. 5 and No. 10 were down; all other reflectors were up.

* Relative to 360°F.

\+ Estimated uncertainty in temperature is ±2.5°F.

TABLE 4 (Continued)

TEMPERATURE-REACTIVITY EFFECT (360-760°F)

(Assembly I-I)

Reading Number	Reflector Position (cm)		Reactor Inlet+ Temperature (°F)	Negative Reactivity* Feedback (cents)
	No. 3	No. 8		
22	72.05	1.03	643	180.8
23	75.51	1.03	651	186.2
24	83.60	1.03	665	193.5
25	94.50	1.03	675	200.0
26	up	8.50	688	207.4
27	up	14.65	700	214.5
28	up	27.48	731	233.8
29	up	28.68	738	235.9
30	up	29.43	740	237.2
31	up	31.86	748	241.6
32	up	32.42	749	242.6
33	up	32.92	750	243.6
34	up	33.88	753	245.4
35	up	34.59	756	246.7
36	up	35.01	758	247.5
37	up	35.27	758	248.0
38	up	35.51	759	248.4
39	up	35.39	759	248.2
40	up	35.39	759	248.2

Reflector No. 5 was down; all other reflectors were up.

* Relative to 360°F.

\+ Estimated uncertainly is ±2.5°F.

D. Experiments in Assembly I-J

1. Coolant Temperature Reactivity:

Experimental Method:

See Item B in 7-SEFOR-1.

Results:

The reactivity effect due to a change in average coolant temperature while holding the power constant was measured at two different power levels during the power ascension phase of the experimental program. The measured results are tabulated in Table 5. The at-power results in Table 5 show that the power calculated from a thermal heat balance and the power indicated by the neutron instrumentation (the wide range monitor - WRM's) tended to diverge as the coolant temperature was decreased below 700°F. The fuel temperatures are shown in Table 5 of 7-SEFOR-1.

2. Reflector Temperature Reactivity:

Experimental Method:

In these experiments the reflector temperature was first increased by decreasing the gas flow around the reflectors and then decreased by increasing the gas flow to its original value. During the measurements a fine reflector position was adjusted to maintain a constant flux level. The average variation in flux level was held to 1 part in 700, while the variation in average core coolant (sodium) temperature during the measurements was held to less than 1°F.

The reflector temperature readings shown in Table 6 were taken from two thermocouples located near the center of coarse reflector #6. This reflector was maintained in completely raised position during the measurement and the thermocouples were in the vicinity of the peak reflector gamma and neutron flux.

Results:

The data of Table 6 indicates that the core reactivity decreases very slightly with increasing reflector temperature, and

that the effect is about -0.01¢/°F. The measured reactivity is of the same magnitude as the previously estimated standard deviation (±0.5¢) in reactivity measurements at zero power. Since the normal change in reflector temperature between zero power and 5 MW is 60°F or less, the reflector temperature coefficient may be treated as zero at power level < 5 MW.

TABLE 5

COOLANT TEMPERATURE REACTIVITY DATA AT A CONSTANT POWER

Date (1970)	Reflector #3 Position (cm)	Reflector #3 Worth (¢)	Reflector #8 Position (cm)	Reflector #8 Worth (¢)	Thermal Power (MW)	Neutron Instrumentation (MW)	Average Coolant Temperature (°F)	Reactivity* Change at a Constant Thermal Power (¢)
7/9-7/24	-	60.82	47.00	69.97	5.1	5.1	760.0	0
7/27	35.53	46.76	0	0	5.2	4.9	604.0	85.3
7/27	36.80	49.12	0	0	5.4	5.1	603.6	85.6
7/27	40.00	56.14	48.00+	70.36	5.4	4.9	500.6	142
7/28	0+	0	51.52+	71.03	5.8	5.1	401.8	202
8/14-8/17	70.00	110.23	-	78.92	10.0	10.2	760.0	0
8/18	0	0	53.77	82.93	10.0	9.5	559.4	106

* Power reactivity corrections were made using a reactivity coefficient of -13¢/MW at 5 MW.

\+ Reflector #10, which as a reactivity worth of 133¢, was completely lowered at the two lower temperature, and was completely raised at the higher temperature.

TABLE 6

REFLECTOR TEMPERATURE-REACTIVITY MEASUREMENTS

Data Set Number	Average Core Temperature (°F)	Reflector Position (cm)	No. 3 Worth+ (¢)	Core Temperature Reactivity** Correction to 760 F (¢)	Reflector Thermocouple No. 56 (°F)	Reflector Thermocouple No. 60 (°F)	Relative*** Reactivity (¢)
1	760.4	42.20	-61.14	+0.22	152	130	+0.11 ± 0.5*
3	759.9	42.17	-61.08	-0.06	149	128	-0.11 ± 0.5*
2	760.8	42.94	-62.56	+0.44	290	252	-1.09 ± 0.5*

* This is the previously estimated standard deviation in a reactivity measurement at zero power. Data are now being collected to obtain an estimate of the deviation at power.

\+ This is the negative reactivity which would be inserted if the reflector were moved to its completely lowered position.

** Core temperature reactivity corrections made using a reactivity coefficient of -0.55¢/°F.

***The relative reactivity was adjusted to make the average of the values for set one and three equal to zero.

Theoretical Analysis

The calculations of the expansion coefficients were performed for two fully loaded cores and one partially loaded core described in Theoretical Analysis of 7-SEFOR-1. All expansion reactivity effects are assumed to vary linearly with respect to the dominating variable, i.e. change(+) in height, radius, etc. These expansion coefficients, listed in Tables 7 and 8, were calculated from the results of a series of 13 energy group two-dimensional synthesis code BISYN.

Figure 1 illustrates the excellent agreement between the predicted temperature dependent reactivity feedback, and the experimentally determined reactivity feedback for Assembly I-E.(++) This agreement is further illustrated in Table 3 where the reactivity coefficients calculated from the predicted total expansion coefficient of -0.36 cent /°F and the predicted Doppler Tdk/dT of -0.0082 is compared with the coefficients determined from a least squares fit of the experimental data. Since the prediction was based on a reactor model containing 19 B_4C rods, while Assembly I-E contained 14 B_4C rods, the calculated values should be modified to reflect this difference. Using the calculated results for 12 B_4C rods as a basis for interpolating to a core with 14 B_4C rods results in about a 4% increase in the calculated total coefficient. Regardless of which calculated coefficients are used, the agreement between calculation and experiment is quite good.

(+) The table of structure thermal expansion coefficients are shown in Reference 9.

(++) Although core loadings, and thus reflector arrangements, were different in Assemblies I-D and I-E, two-dimensional synthesis calculations which were performed to estimate the influence of reflector density on the temperature coefficients of reactivity indicated that only one or two percent difference in the total coefficient was found in the two assemblies.

TABLE 7

EXPANSION REACTIVITY COEFFICIENTS FOR FULLY LOADED SEFOR CORE

Effect	Percentage Change** per degree Fahrenheit (%/°F)	Reactivity Effects* for Core with 19 B_4C Rods (¢/°F)
Fuel Axial Expansion	+0.000461	-0.009+
Fuel Clad Axial Expansion	+0.000980	-0.072+
BeO Axial Expansion	+0.000580	-0.003
Structure Axial Expansion	+0.000980	-0.014
Structure Radial Expansion	+0.000980	-0.135
Sodium Density in Core and Axial Reflector	-0.015789	-0.072(-0.076)
Sodium Density Between Core and Vessel	-0.015789	-0.056(-0.059)
B_4C Axial Expansion	+0.000250	+0.002(+0.001)
		-0.359(-0.367)

* If different, the reactivity effect for a core containing 12 B_4C rods is enclosed in parenthesis.

** This represents the percentage change in length, density, etc.

\+ Based on the calculated coefficients in Reference 9 of -19.27¢/% Δh/h for fuel axial expansion and -73.31¢/% Δh/h for fuel clad axial expansion.

TABLE 8

EXPANSION REACTIVITY COEFFICIENTS FOR 512 ROD CORE

Effect	Percentage change** per degree Fahrenheit (%/°F)	Reactivity Effect (c/°F)
Fuel Axial Expansion	+0.000461	-0.009*
Fuel Clad Axial Expansion	+0.000980	-0.072*
BeO Axial Expansion	+0.000580	-0.004
Structure Axial Expansion	+0.000980	-0.014
Structure Radial Expansion	+0.000980	-0.130
Sodium Density in Core and Axial Reflector	-0.015789	-0.093
Sodium Density Between Core and Vessel	-0.015789	-0.122
B_4C Axial Expansion	+0.000250	0.0
		-0.444

* Based on the calculated coefficients in Reference 9 of -19.27¢/% Δh/h for fuel axial expansion and -73.31¢/% Δh/h for fuel clad axial

** This represents the percentage change in length, density, etc.

8 - SEFOR-1 (cont'd)

References

1. L.D. Noble et al., GEAP-13588 (March, 1970) pp.127-160
2. R.A. Meyer et al., GEAP-13598 (June, 1970) pp.3.42-3.77
3. GEAP-10010-20 (Feb. - April, 1969) pp.9-10
4. GEAP-10010-21 (May - July, 1969) pp.45-49
5. GEAP-10010-22 (Aug. - Oct., 1969) pp.21-24
6. GEAP-10010-23 (Nov., 1969 - Jan., 1970) pp.20-21
7. GEAP-10010-24 (Feb. - April, 1970) p.21
8. GEAP-10010-25 (May - July, 1970) pp.6-14
9. GEAP-10010-26 (Aug. - Oct., 1970) pp.15-37
10. GEAP-10010-27 (Nov., 1970 - Jan., 1971) pp.12-14

9 - SEFOR-1 Flow and Pressure Coefficient of Reactivity

Facility: SEFOR Assembly: I

A. Experiment in Assembly I-E

Experimental Method:

In pressure-reactivity measurements the vessel cover gas pressure was changed from zero to 20 psig at 350°F*. In flow-reactivity measurements the coolant flow was changed from 370 gpm to 4,000 gpm at 350°F* and from 500 gpm to 4,900 gpm at 400°F*. The variation in reactor temperature during these measurements was held to 20°F or less.

*) core temperature

Results:

The flow and pressure coefficient of reactivity are essentially zero. The reactivity effects that are associated with changes over the normal operating range of reactor vessel hydraulic pressure and primary coolant flow are of the order of the standard deviation (0.5¢) in reactivity difference measurement.

Reference:

1. L.D. Noble et al., GEAP-13588 (March 1970) pp.127-129

Facility: SEFOR (1. SEFOR) Assembly: 1 (2. SEFOR-1)

1. L.D. Noble, F. Mitzel, B. Sarma, D. Wintzer, Y.S. Lu, G. Kessler, G.R. Pflasterer, R.A. Becker and L. Mansur, Results of SEFOR Zero Power Experiments, GEAP-13588, March 1970

2. R.A. Meyer, A.B. Reynolds, S.L. Stewart, M.L. Johnson and E.R. Craig, Design and Analysis of SEFOR Core I, GEAP-13598, June 1970

3. L.D. O'Dell, Calculation of the Isothermal Doppler Coefficient for the Southwest Experimental Fast Oxide Reactor (SEFOR), HEDLTME 71-81, May 1971

4. L.D. Noble and C.D. Wilkinson, Final Specifications for the SEFOR Experimental Program, GEAP-5576, January 1968

5. G.I. Bell, A Single Treatment for Effective Resonance Absorption Cross Sections in Dense Lattices, Nucl. Sci. Eng. 5, P.138, 1959

6. B.A. Hutchins, The ENDRUN code- General Description, G.E.-BRDO Memo, June 11, 1968

7. P. Greebler, et al, "BISYN- A Two-Dimensional Synthesis Program", GEAP-4922, July 1965

8. R. Protsik and E.G. Leff, Users Manual for DOT2DB: A Two Dimensional Multigroup Discrete Ordinated Transport/Diffusion code with Anisotropic scattering, GEAP-13537 September 1969

9. Wilkinson, D., "Weighted Doppler Analysis Code-WEDOP" GEAP-5513, October 1967

Southwest Experimental Fast Oxide Reactor Development Program

10. Thirteenth Quarterly Report, May-July 1967, GEAP-5533, August 1967 PP.21-26

11. Nineteenth Quarterly Report, November 1968-January 1969, GEAP-5754, February 1969 PP.35-43

12. Twentieth Quarterly Report, February-April 1969, GEAP-10010-20, May 1969 PP.9-11

13. Twenty-first Quarterly Report, May-July 1969, GEAP-10010-21, August 1969 P.37, PP.45-50

15 - SEFOR-1 (cont'd)

14. Twenty-second Quarterly Report, August-October 1969, GEAP-10010-22, November 1969 PP.21-31

15. Twenty-third Quarterly Report, November 1969-January 1970, GEAP-10010-23, February 1970 PP.20-26

16. Twenty-fourth Quarterly Report, February-April 1970, GEAP-10010-24, May 1970 PP.21-45

17. Twenty-fifth Quarterly Report, May-July 1970, GEAP-10010-25, August 1970 PP.6-14

18. Twenty-sixth Quarterly Report, August-October 1970, GEAP-10010-26, November 1970 PP.15-37

19. Twenty-seventh Quarterly Report, November 1970-January 1971, GEAP-10010-27, February 1971 PP.12-14

16 - SEFOR-1 Experimental References

Facility: SEFOR (1-SEFOR) Assembly: 1 (2-SEFOR-1)

1. L.D. Noble, F.Mitzel, B. Sarma, D. Wintzer, Y.S. Lu, G. Kessler, G.R. Pflasterer, R.A. Becker, L.Mansur, Results of SEFOR Zero Power Experiments, GEAP-13588, AEC Research and Development Report. March, 1970.

2. G.R. Pflasterer et al., Investigation of Low Plutonium Content in SEFOR Fuel, GEAP-13576

3. R.A. Meyer, A.B. Reynolds, S.L. Stewart, M.L. Johnson, and E.R. Craig, Design and Analysis of SEFOR Core I, GEAP-13598, June, 1970.

4. E.R. Craig, SEFOR Instrumented Fuel Assembly Design and Development, GEAP-5615, AEC Research and Development Report, April, 1968.

5. L.D. Noble and C.D. Wilkinson, Final Specification for the SEFOR Experimental Program, GEAP-5576, AEC Research and Development Report, January, 1968.

6. G.R. Keepin, "Physics of Nuclear Kinetics", Addison Wesley, 1965.

Southwest Experimental Fast Oxide Reactor Development Program

7. Thirteenth Quarterly Report, May-July, 1967, GEAP-5533, August, 1967.

8. Nineteenth Quarterly Report, November 1968-January 1969, GEAP-5754, February 1969.

9. Twentieth Quartery Report, February-April 1969, GEAP-10010-20, May 1969.

10. Twenty-first Quartery Report, May-July 1969, GEAP-10010-21, August, 1969.

11. Twenty-second Quartery Report, August-October, 1969, GEAP-10010-22, November, 1969.

12. Twenty-third Quartery Report, November 1969-January 1970, GEAP-10010-23, February, 1970

13. Twenty-fourth Quartery Report, February-April 1970, GEAP-10010-24, May, 1970.

16 - SEFOR-1 (cont'd)

14. Twenty-fifth Quartery Report, May-July 1970, GEAP-10010-25, August, 1970.

15. Twenty-sixth Quartery Report, August-October, 1970, GEAP-10010-26, November, 1970.

16. Twenty-seventh Quartery Report, November, 1970-January, 1971, GEAP-10010-27, February, 1971.